Journal of Power Sources 581 (2023) 233500

Contents lists available at ScienceDirect

Journal of Power Sources

journal homepage: www.elsevier.com/locate/jpowsour

Beyond traditional boundaries: Exergo-economic and thermo-mechanical optimization of segmented thermoelectric generators with varied cross-sections

Hisham Alghamdi [a], Chika Maduabuchi [b,c,*], Kingsley Okoli [c,d], Abdullah Albaker [e], Ibrahim Alatawi [f], Mohammed Alghassab [g,**], Hind Albalawi [h], Mohammad Alkhedher [i]

[a] Electrical Engineering Department, College of Engineering, Najran University, Najran, 55461, Saudi Arabia
[b] Department of Nuclear Science and Engineering, Massachusetts Institute of Technology, Cambridge, MA, USA
[c] Artificial Intelligence Laboratory, University of Nigeria Nsukka, Nsukka, 410001, Enugu, Nigeria
[d] Department of Computer Science and Knowledge Discovery, Saint Petersburg Electrotechnical University LETI, Saint Petersburg, 197022, Russia
[e] Department of Electrical Engineering, College of Engineering, University of Ha'il, Ha'il, 81451, Saudi Arabia
[f] Department of Mechanical Engineering, College of Engineering, University of Ha'il, Ha'il, 81451, Saudi Arabia
[g] Electrical Engineering Department, College of Engineering, Shaqra University, Riyadh, 11911, Saudi Arabia
[h] Department of Physics, College of Sciences, Princess Nourah bint Abdulrahman University (PNU), P.O. Box 84428, Riyadh, 11671, Saudi Arabia
[i] Department of Mechanical and Industrial Engineering, Abu Dhabi University, Abu Dhabi, 59911, United Arab Emirates

HIGHLIGHTS

- Investigated optimizing a solar trapezoidal-segmented thermoelectric generator.
- Optimal 6.17% skutterudite for peak power (47.47 W) and exergy efficiency (10.95%).
- Optimal power conditions result in maximized CO_2 savings per year (22.5 $kgyr^{-1}$).
- Optimal semiconductor height of 0.2 mm minimizes dollar per watts to 0.0048 $\$W^{-1}$.
- Minimum thermal stress (0.25 GPa) achieved at 4 kWm^{-2} K^{-1} heat transfer coefficient.

ARTICLE INFO

Keywords:
Concentrating solar segmented thermoelectric generator
Variable area leg geometry
Solar heat flux
Cooling film coefficient
Comprehensive performance optimization

ABSTRACT

In this work, we present a comprehensive optimization study of a concentrating solar segmented thermoelectric generator (CSSTEG) with variable area leg geometry. We consider not just geometrical parameters but also concentrated solar heat flux and convective cooling film coefficients, pushing the boundaries of traditional studies. Performance is evaluated on multiple fronts: power output, exergy efficiency, entropy generation, CO_2 savings, dollar per watt, and thermal stress. Uniquely, we establish that an optimal skutterudite content of 6.17% provides maximum power output (47.47 W) and exergy efficiency (10.95%) at a solar heat flux of 50 kWm^{-2}. This optimized configuration also delivers maximal annual CO_2 savings (22.5 $kgyr^{-1}$). Additionally, we pinpoint that a semiconductor height of 0.2 mm minimizes the dollar per watt (0.0048 $\$W^{-1}$) at 100 kWm^{-2} solar irradiances and reduces thermal stress (0.25 GPa) at a cooling heat transfer coefficient of 4 kWm^{-2} K^{-1}. Our research is pioneering in its holistic approach to CSSTEG optimization, providing valuable insights for creating efficient, sustainable energy systems.

1. Introduction

In light of escalating global energy demand, coupled with increasing concerns over climate change, the transition to sustainable, eco-friendly power generation technologies is of paramount importance. Traditionally, the lion's share of the world's energy demand has been met through

* Corresponding author. Department of Nuclear Science and Engineering, Massachusetts Institute of Technology, Cambridge, MA, USA.
** Corresponding author.
E-mail addresses: chika691@mit.edu, chika.maduabuchi.191341@unn.edu.ng (C. Maduabuchi), malghassab@su.edu.sa (M. Alghassab).

https://doi.org/10.1016/j.jpowsour.2023.233500
Received 13 July 2023; Received in revised form 29 July 2023; Accepted 7 August 2023
Available online 17 August 2023

fossil fuels, causing severe environmental degradation and health problems [1]. Moreover, fossil fuel reserves are finite and their extraction and usage have considerable economic implications, including price volatility, geopolitical issues, and long-term unavailability [2–4].

In contrast, renewable energy, especially solar power, offers a promising and virtually inexhaustible alternative with fewer environmental, health, and economic issues. In particular, Concentrating Solar Thermoelectric Generators (CSTEGs) [5,6] have emerged as a viable and innovative solution to meet our growing energy needs sustainably. This technology taps into the thermoelectric effect, transforming concentrated solar radiation into electrical energy, exhibiting promising efficiencies and minimized greenhouse emissions. Despite notable research endeavors targeting improved device efficiency via modification of thermoelectric material properties [7], geometry optimization [8], multi-stage configurations [9], and hybrid system operation [10], considerable potential remains untapped.

One of the key strategies for optimizing device performance, particularly under high-temperature scenarios such as concentrated solar energy [11] or full-load automotive exhaust [12] applications, is the segmentation of materials in the thermoelectric pins [13]. Since the pioneering development of the segmented thermoelectric generator (STEG) by Ioffe et al. [14], significant strides have been made in evolving this technology.

Recent developments include Liu et al. [15], who used a transient model combined with neural networks to study parameter matching and heat conduction for optimizing performance and reliability. Zhu et al. [16] crafted a prediction model for STEGs using iterative-training-based artificial neural networks, which expedite the analysis and design process. Shittu et al. [17] performed an in-depth analysis of energy and thermo-mechanical performance under non-uniform solar irradiance, emphasizing the influence of thermoelectric pin geometry on device performance. Yu et al. [18] inspected power production and thermal stress in STEGs under pulsed heating conditions, suggesting that high thermal stress can be mitigated with thicker solder pads. Similarly, Chen et al. [19] leveraged evolutionary computational algorithms and the finite element method to enhance the electrical performance of STEG thermocouples. These advancements affirm the superiority of STEGs over traditional TEGs for high-temperature applications.

Despite these significant contributions, the findings predominantly stem from models that rely on uniform cross-sectional area thermoelements, an approach that inadvertently restricts device performance. This unaddressed limitation underscores the necessity for further exploration into the performance enhancement potential of segmented materials within non-uniform cross-sectional shaped thermoelements for TEGs. It paves the way for novel research that holistically considers different thermoelement geometries to advance TEG performance.

Despite remarkable advancements in STEG technology, prior research including that by Liu et al. [15], Zhu et al. [16], Shittu et al. [17], Yu et al. [18], and Chen et al. [19], predominantly relied on uniform cross-sectional area thermoelements, which inadvertently restricts device performance [20], motivating the exploration of non-uniform cross-sectional shaped thermoelements [21]. For instance, investigations by Olivares-Robles et al. [22], Luo et al. [23], Shittu et al. [24], and Zhang et al. [25], have provided significant insights into optimizing energy and power output of segmented, variable cross-sectional area thermoelements, but they often neglect the comprehensive evaluation of these devices which introduces the novelties of this work.

The novelty of our work resides in its integrative approach, offering a thorough environmental, economic, and thermo-mechanical assessment of a full-scale thermoelectric module, composed of 127 segmented, variable cross-sectional area thermocouples. We further enhance the accuracy of our study by considering the devices under diverse, dynamic heat fluxes and cooling heat transfer coefficients, rather than static conditions. Moreover, this research accounts for mutual electrical and thermal interactions between the thermocouples, an aspect generally overlooked in conventional studies. Therefore, our research extends the frontiers of TEG studies, delivering significant strides toward optimized performance under high-temperature scenarios such as concentrated solar energy or full-load automotive exhaust applications. By addressing these gaps in existing research, our work promises to advance the understanding and application of segmented thermoelectric.

In this study, we present an unprecedented, comprehensive exploration of segmented variable area leg TEGs (SVAL-TEGs). Drawing on and advancing the state-of-the-art research, we conduct a robust and all-inclusive analysis, factoring in not only energy and exergy considerations but also incorporating entropy, environmental, economic, and thermo-mechanical optimization aspects. Our approach is applied to a full-scale SVAL-TEG module that comprises 127 distinct segmented thermoelectric couples, each with variable area leg geometries.

Our research does not stop at a static analysis. Instead, it optimizes the comprehensive performance of the device under dynamic concentrated heat fluxes and convective film coefficients. The optimization parameters include the height of the semiconductor, its cross-sectional area, and the amount of skutterudite involved. This detailed approach paints a more realistic picture of the SVAL-TEG performance under diverse operational conditions, providing a concrete optimization guide for future device manufacturing.

Furthermore, we harness the power of advanced computational modeling through a three-dimensional finite element model implemented in the ANSYS software. This allows for the nuanced consideration of temperature dependency across all 508 thermoelectric semiconductors used to model the realistic module. Notably, this level of detail is uncharted territory in current literature, as prior works have not typically taken into account the influence of optimized parameters under fluctuating heat fluxes and convective cooling heat transfer coefficients.

By connecting the theoretical aspects of our work to practical applications, we anticipate that our findings will not only advance the scientific understanding of SVAL-TEGs but also inform the manufacturing process of these cutting-edge devices. In particular, we foresee this research contributing significantly to the development of novel thermoelectric modules through three-dimensional printing techniques. This synthesis of complex theoretical analysis and practical, manufactural insights sets our work apart and should be of great interest to researchers and industry professionals alike in the field of power sources.

The remainder of this paper is structured as follows: Section 2 provides an illustrative depiction of the full-scale module. Given the complexity and breadth of the governing equations of thermoelectric phenomena, we've relegated their detailed explanation, their validation through comparisons with prior studies, and the specifics of the boundary conditions defining the numerical model to the supplementary material accompanying this work. This approach allows for a more concise and focused main manuscript. Following this, Section 3 delves into the presentation and discussion of our results. Finally, Section 4 encapsulates the major conclusions derived from this study's robust results.

2. Methods

This section presents an overview of the methodology used in optimizing the performance of the segmented variable area leg thermoelectric generator. First, a conceptualized model of the thermoelectric module is presented alongside the dimensions of all components in Fig. 1. Second, the equations governing the finite element method used to study the optimal parameters of the system are discussed alongside the boundary conditions used to virtually define the model. Finally, the verification of the numerical method is carried out by comparing the results obtained with similar results from previous studies.

To realize the objective of this study, a three-dimensional model of the thermoelectric module is developed using the Autodesk Inventor

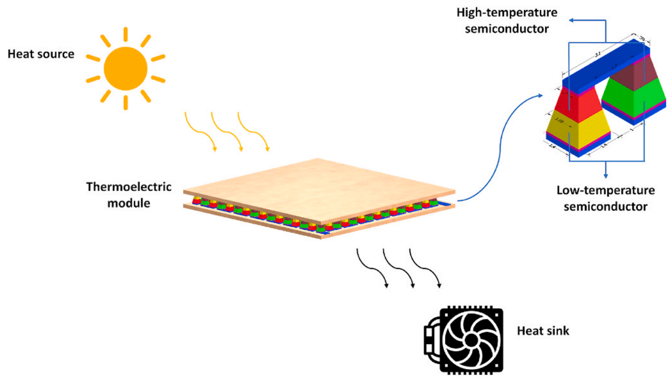

Fig. 1. Pictorial description of the system. All units are provided in mm.

Professional 2023 software. A pictorial representation of the computer aided design model of the system is shown in Fig. 1 as well as the dimensions of all components of the system. To obtain practical results, the dimensions of the components are obtained from a thermoelectric module manufactured by Melcore ™ in the USA which was used in a previous study [26]. All dimensions of the thermoelectric module are provided in mm.

Further information on the methodology including the description of the component materials' properties, the three-dimensional field equations, the boundary conditions, the performance equations, and verification of the numerical model is provided in section 1 of the Supplementary Material accompanying this work.

3. Results and discussion

This section portrays and discusses the results obtained from the parametric energy, exergy, entropy, environmental, economic, and thermo-mechanical study of the solar segmented thermoelectric generator with variable area leg geometry configuration. Since the heating and cooling conditions affect the performance of the device most significantly, the combined effects of concentrated solar irradiance and cold junction convective film coefficient as well as the geometry parameters of the semiconductor pellets which include the: height, cross-sectional area (CSA), amount of skutterudite, and cross-sectional area ratio between *n*- and *p*-type semiconductors. This comprehensive analysis is enough to give the designer a detailed overview of the necessary optimums needed to manufacture a high performing, environmentally

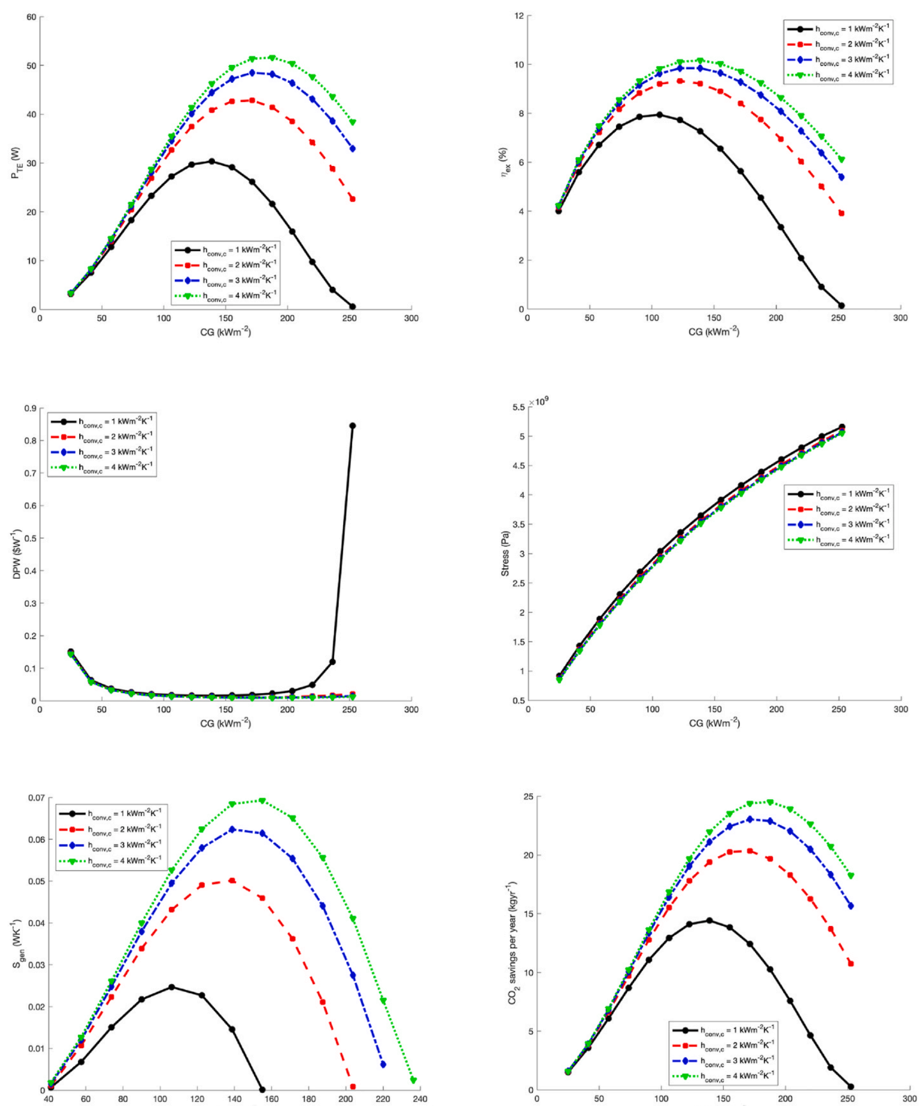

Fig. 2A. Effects of concentrated solar irradiance on power output, exergy efficiency, entropy generation, CO2 savings per year, dollars per watts, and thermal stress in the thermoelectric generator system.

friendly, economically viable, and long-lasting thermoelectric device.

3.1. Concentrated solar irradiance and convective cooling film coefficient

In Fig. 2A, a comprehensive analysis was conducted to investigate the relationship between concentrated solar irradiance and various system parameters under constant boundary conditions. The concentrated solar irradiance was varied within the range of 0–300 kWm^{-2}. The results revealed distinct optimal values for each parameter at different concentration ratios, offering valuable insights for the optimization and design of the SVAL-TEG system. The power output demonstrated a maximum value of 51.62 W at a solar concentration irradiance of 187.5 kWm^{-2} (Fig. 3a), indicating the highest achievable electrical power output at 4 kWm^{-2} K^{-1} convective cooling film coefficient. Similarly, the exergy efficiency exhibited its peak performance at a concentrated solar irradiance of 138.75 kWm^{-2}, reaching 10.16%. This indicates the system's ability to convert solar energy into useful work efficiently. The analysis also revealed the concentrated solar irradiance at which entropy generation was highest, which was found to be 155 kWm^{-2} with a value of 0.069 WK^{-1}. This indicates the extent of thermodynamic irreversibility and system inefficiency at that concentration ratio. On the other hand, the maximum annual CO_2 savings of 24.52 kgyr^{-1} were observed at a concentrated solar irradiance of 187.5 kWm^{-2}, emphasizing the environmental benefits of the system. The dollar per watt ratio, a measure of the economic efficiency, reached its peak of 0.84 \$W^{-1} at a concentrating solar irradiance of 252.5 kWm^{-2}. This implies that the system achieved the highest cost-effectiveness at other concentrating solar irradiances below this value. Additionally, thermal stress experienced a rapid increase, reaching 5.16 GPa at a concentrating solar irradiance of 252.5 kWm^{-2}. This highlights the mechanical strain on the system components and the importance of considering thermal stress in the system design. It is noteworthy that the cold junction convective film coefficients played a significant role in determining the performance of different parameters. Higher coefficients of 4 kWm^{-2} K^{-1} were favorable for power output, exergy efficiency, and CO_2 savings per year, whereas the minimum coefficients of 1 kWm^{-2} K^{-1} were preferred for managing thermal stress. These findings provide crucial insights into concentrating solar irradiance that optimize power output, exergy efficiency, CO_2 savings, and economic viability. Moreover, the understanding of concentration-dependent behavior for entropy generation and thermal stress contributes to identifying operational limits and potential system failures. This finding contributes to the development of efficient and reliable solar concentration systems, enhancing overall performance and environmental

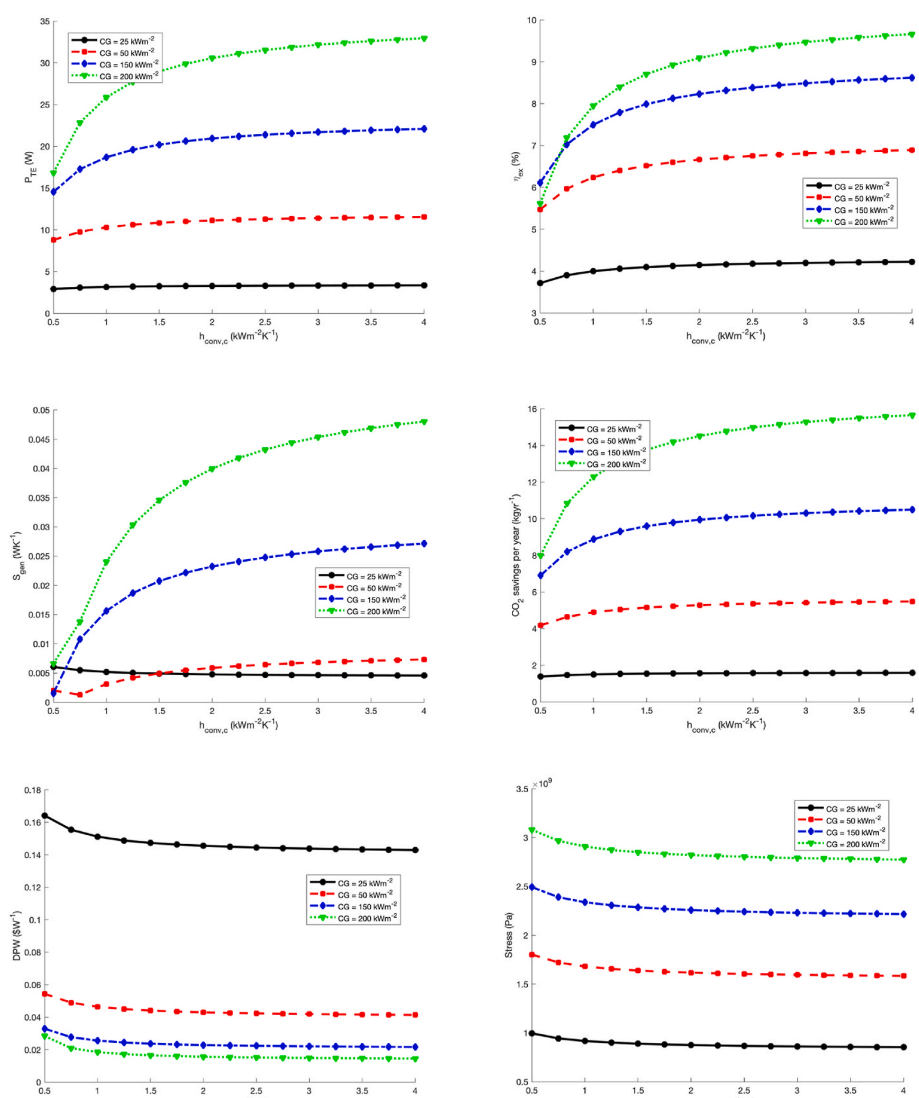

Fig. 2B. Effects of convective cooling film coefficient on power output, exergy efficiency, entropy generation, CO2 savings per year, dollars per watts, and thermal stress in the thermoelectric generator system.

sustainability.

The comprehensive analysis of the relationship between concentrated solar irradiance and various system parameters in Fig. 2A provides crucial insights for optimizing and designing the SVAL-TEG system. The identified optimal values for power output, exergy efficiency, CO2 savings, and dollar per watt ratio at specific concentration ratios underscore the importance of selecting appropriate solar irradiance levels for maximum performance and economic efficiency. Additionally, the understanding of concentration-dependent behavior for entropy generation and thermal stress informs operational limits and facilitates the development of more efficient and reliable solar concentration systems, ultimately enhancing overall system performance and environmental sustainability.

The present study investigated the impact of the convective cooling film coefficient on the performance parameters of a system and the results are depicted in Fig. 2B. By varying the convective cooling film coefficient within the range of 0.5–4 $kWm^{-2}\,K^{-1}$ under different levels of concentrated solar irradiation (25, 50, 150, and 200 kWm^{-2}), several effects were observed. The power output of the system exhibited an increasing trend with the cooling coefficient, reaching maximum power output of 3.34 W, 11.54 W, 22.09 W, and 32.94 W at a convective cooling coefficient of 4 $kWm^{-2}\,K^{-1}$ for solar irradiances of 25, 50, 150, and 200 kWm^{-2}, respectively. Similarly, the exergy efficiency demonstrated peaks of 4.22%, 6.89%, 8.61%, and 9.65% at a convective cooling film coefficient of 4 $kWm^{-2}\,K^{-1}$ for the corresponding concentrating solar irradiances. Entropy generation exhibited variations with the cooling coefficient, with maximum values of 0.004 WK^{-1}, 0.007 WK^{-1}, 0.027 WK^{-1}, and 0.048 WK^{-1} observed at a convective cooling coefficient of 4 $kWm^{-2}\,K^{-1}$ for different concentrating solar irradiances. However, at a concentrating solar irradiation of 50 kWm^{-2}, entropy initially decreased at a convective cooling coefficient of 0.5 kWm^{-2} before rising to 0.006 WK^{-1}. CO_2 savings per year showed a doubling effect as the cooling coefficient increased from 0.5 to 4 $kWm^{-2}\,K^{-1}$ at a concentrated solar irradiation of 200 kWm^{-2}, reaching 15.64 $kgyr^{-1}$. Conversely, at a concentrated solar irradiation of 25 kWm^{-2}, CO_2 savings demonstrated slight progress but remained linear throughout the convective cooling process. The dollar per watt values exhibited variations, with the highest value observed at 0.164 $\$W^{-1}$ for a cooling coefficient of 0.5 $kWm^{-2}\,K^{-1}$ and a solar irradiation of 25 kWm^{-2}. Subsequently, this value decreased to 0.143 $\$W^{-1}$. For solar irradiances of 50, 150, and 200 kWm^{-2}, the dollar per watt values were 0.054 $\$W^{-1}$, 0.032 $\$W^{-1}$, and 0.028 $\$W^{-1}$ respectively. These values provide insights into the economic aspect of the system, indicating the cost-effectiveness of power generation at different cooling coefficients and solar irradiances. Thermal stress demonstrated maximum values of 3.08 GPa, 2.49 GPa, 1.8 GPa, and 0.99 GPa at a convective cooling coefficient of 0.5 $kWm^{-2}\,K^{-1}$ for concentrating solar irradiances of 200, 150, 50, and 25 kWm^{-2}, respectively. The results highlight the influence of the convective cooling film coefficient on the performance of the TEG system. The findings indicate that increasing the cooling coefficient leads to higher power output, exergy efficiency, and CO_2 savings. The maximum values for these parameters were observed at a convective cooling coefficient of 4 $kWm^{-2}\,K^{-1}$. This implies that selecting an appropriate cooling coefficient can significantly optimize the system's performance in terms of power generation, efficiency, and environmental benefits. These findings provide valuable insights for the design and operation of solar energy systems.

The investigation of the convective cooling film coefficient's impact on the thermoelectric generator system parameters in Fig. 2B reveals essential insights for system optimization. The observed increasing trends in power output, exergy efficiency, and CO_2 savings with higher cooling coefficients demonstrate the potential for enhancing system performance and environmental benefits by selecting appropriate cooling values. The findings highlight the significance of convective cooling in improving power generation and efficiency, providing valuable guidance for designing and operating solar energy systems. Optimizing the cooling coefficient can lead to higher power output and efficiency, contributing to the overall sustainability and effectiveness of the thermoelectric generator system.

3.2. Semiconductor height

From Fig. 3A, the analysis of power output revealed distinct patterns for different concentrated solar irradiance levels and semiconductor heights. At higher solar irradiance (200 kWm^{-2}), the power output initially increased with semiconductor height, reaching a maximum at 1.2 mm before experiencing a sudden drop and then declining steeply. This suggests that there exists an optimal semiconductor height for maximizing power output. At lower solar irradiance levels (150 kWm^{-2}, 50 kWm^{-2}, and 25 kWm^{-2}), similar trends were observed, with power output reaching a peak and then decreasing. These findings highlight the importance of selecting the appropriate semiconductor height to achieve optimal power generation. The findings from the analysis reveal a strong correlation between the exergy efficiency of the system and two key factors: the level of concentrated solar irradiance and the height of the semiconductor material. It is evident that the exergy efficiency is significantly influenced by variations in these parameters. At a solar irradiance level of 50 kWm^{-2}, the system demonstrated its highest exergy efficiency, reaching an impressive value of 10.63%. This indicates that this specific level of solar irradiance is most favorable for converting energy into useful work, maximizing the system's overall efficiency. On the other hand, the lowest exergy efficiency of 0.8% was observed at a solar irradiance level of 25 kWm^{-2}. This suggests that lower levels of solar irradiance are less conducive to efficient energy conversion in the system, resulting in reduced overall performance. Additionally, all the maximum efficiencies were obtained at a semiconductor height of 14.2 mm, emphasizing the importance of optimizing the height to enhance exergy efficiency. The plot also exhibited a wave-like pattern across different concentrated solar irradiance levels. The maximum entropy generation was observed at a solar irradiance of 200 kWm^{-2}, indicating that higher irradiance levels contribute to greater entropy production. Conversely, the least entropy generation was observed at 25 kWm^{-2}. The semiconductor height of 14.2 mm consistently corresponded to the highest entropy generation, indicating that this height may contribute to increased entropy production. Managing and minimizing entropy generation is crucial for improving the system's overall efficiency and reducing losses. The CO_2 savings was influenced by both concentrated solar irradiance and semiconductor height. Higher solar irradiance levels resulted in greater CO_2 savings, with the highest savings observed at 200 kWm^{-2} concentrated solar irradiance. However, the effect of semiconductor height on CO_2 savings was more complex. While a smaller height of 1.2 mm led to the highest CO_2 savings at 200 kWm^{-2} concentrated solar irradiance. The highest savings at the least concentrated solar irradiance of 25 kWm^{-2} were achieved at a height of 5.2 mm. The highest savings in the system decreased to 3.05 $kgyr^{-1}$ at a height of 14.2 mm. These findings indicate that optimizing both solar irradiance and semiconductor height is important for maximizing CO_2 savings. The economic viability of the system, represented by dollars per watt, varied with concentrated solar irradiance and semiconductor height. The highest value was observed at 25 kWm^{-2}, indicating that this irradiance level provided the least economic power generation. The lowest value was obtained at 50 kWm^{-2} and 150 kWm^{-2}. Interestingly, all the lowest values were consistently observed at a semiconductor height of 14.2 mm. These results suggest that careful consideration of both solar irradiance and semiconductor height is necessary to optimize the economic viability of the system. Thermal stress is an important factor to consider in the design and operation of solar systems. The results revealed that higher concentrated solar irradiance levels led to greater thermal stress. The maximum stress was observed at 200 kWm^{-2} concentrated solar irradiance, indicating that this irradiance level poses the highest risk of thermal stress-related issues. The semiconductor height of 14.2 mm was associated with the highest stress levels at all

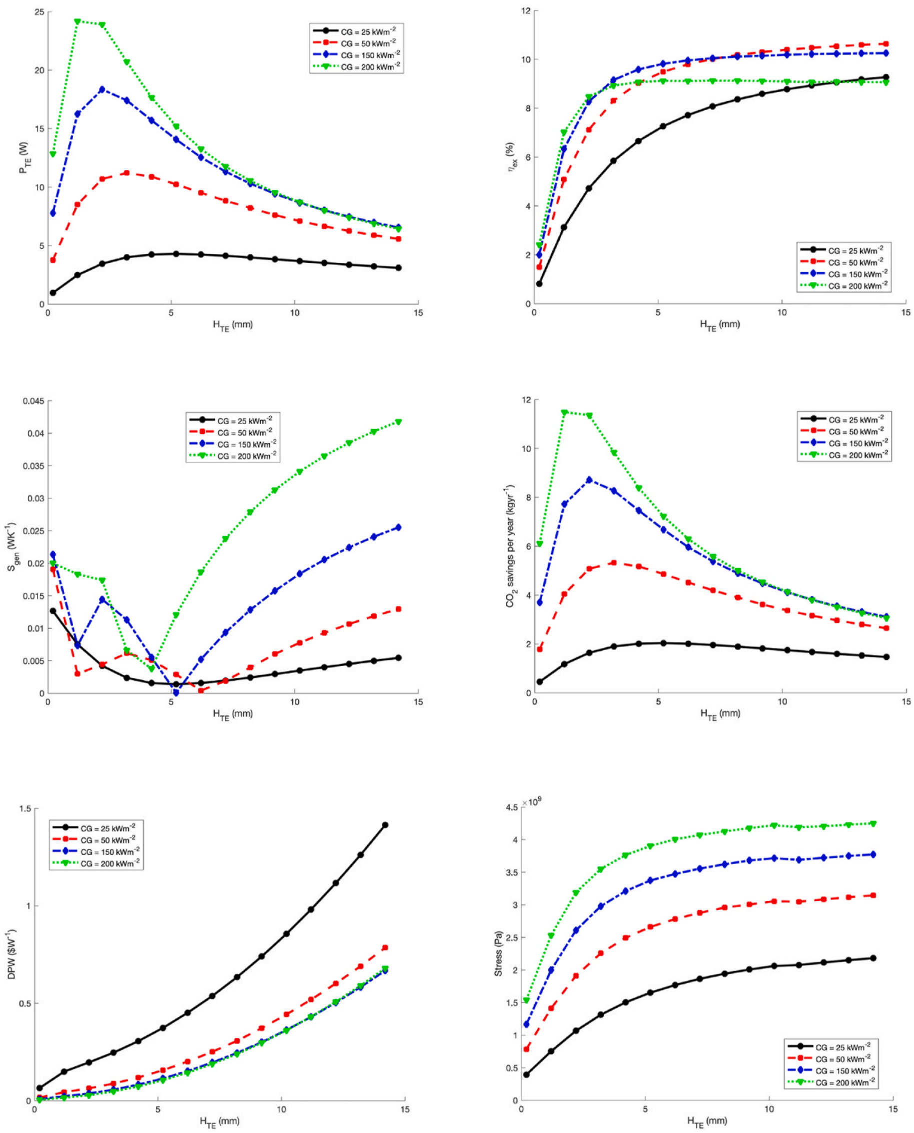

Fig. 3A. Effects of semiconductor height for various concentrated solar irradiance on power output, exergy efficiency, entropy generation, CO2 savings per year, dollars per watts, and thermal stress in the thermoelectric generator system.

irradiance levels. Managing and mitigating thermal stress is essential to ensure the structural integrity and longevity of the system. The plot highlights the complex interplay between concentrated solar irradiance and semiconductor height.

Fig. 3A's analysis highlights the crucial influence of both concentrated solar irradiance and semiconductor height on the thermoelectric generator system's performance. Optimizing the semiconductor height is essential for achieving maximum power output and exergy efficiency, as observed from the distinct patterns at different irradiance levels. Furthermore, managing and minimizing entropy generation and thermal stress, as influenced by both parameters, are crucial for enhancing system efficiency and durability. These findings emphasize the need for a careful and balanced approach to selecting the appropriate solar irradiance and semiconductor height to optimize the system's overall performance and environmental sustainability.

Fig. 3B shows the behavior of the power output. The power output of the system reached its peak at a semiconductor height of 5.2 mm, with a maximum value of 4.53 W. Subsequently, the power output gradually decreased to 3.19 W at a semiconductor height of 14.2 mm across all convective cooling film coefficients. Higher semiconductor heights resulted in reduced power output. The system achieved its maximum exergy efficiency of 9.47% at a semiconductor height of 14.2 mm, exhibiting consistent behavior across all convective cooling film coefficients. Higher semiconductor heights corresponded to improved exergy efficiency. The entropy generation demonstrated an unstable pattern. Initially, at a semiconductor height of 0.2 mm, the system experienced higher entropy generation of 0.012 WK^{-1}. However, as the semiconductor height increased to 5.2 mm, the entropy generation decreased significantly to 0.0005 WK^{-1}. Subsequently, there was a gradual increase to 0.005 WK^{-1} at a semiconductor height of 14.2 mm for all convective cooling film coefficients. The unstable pattern of entropy generation necessitates caution when designing and operating TEG systems. It indicates that small changes in semiconductor height can have a significant impact on system performance. This finding emphasizes the importance of conducting thorough analyses and simulations to identify the optimal operating conditions and semiconductor height that led to desirable performance outcomes, including reduced entropy generation and increased efficiency. The maximum CO_2 savings per year were observed at a semiconductor height of 5.2 mm, reaching 2.15 $kgyr^{-1}$. As the semiconductor height increased to 14.2 mm, the CO_2 savings decreased to 1.51 $kgyr^{-1}$ for all convective cooling film coefficients. Higher semiconductor heights resulted in reduced CO_2

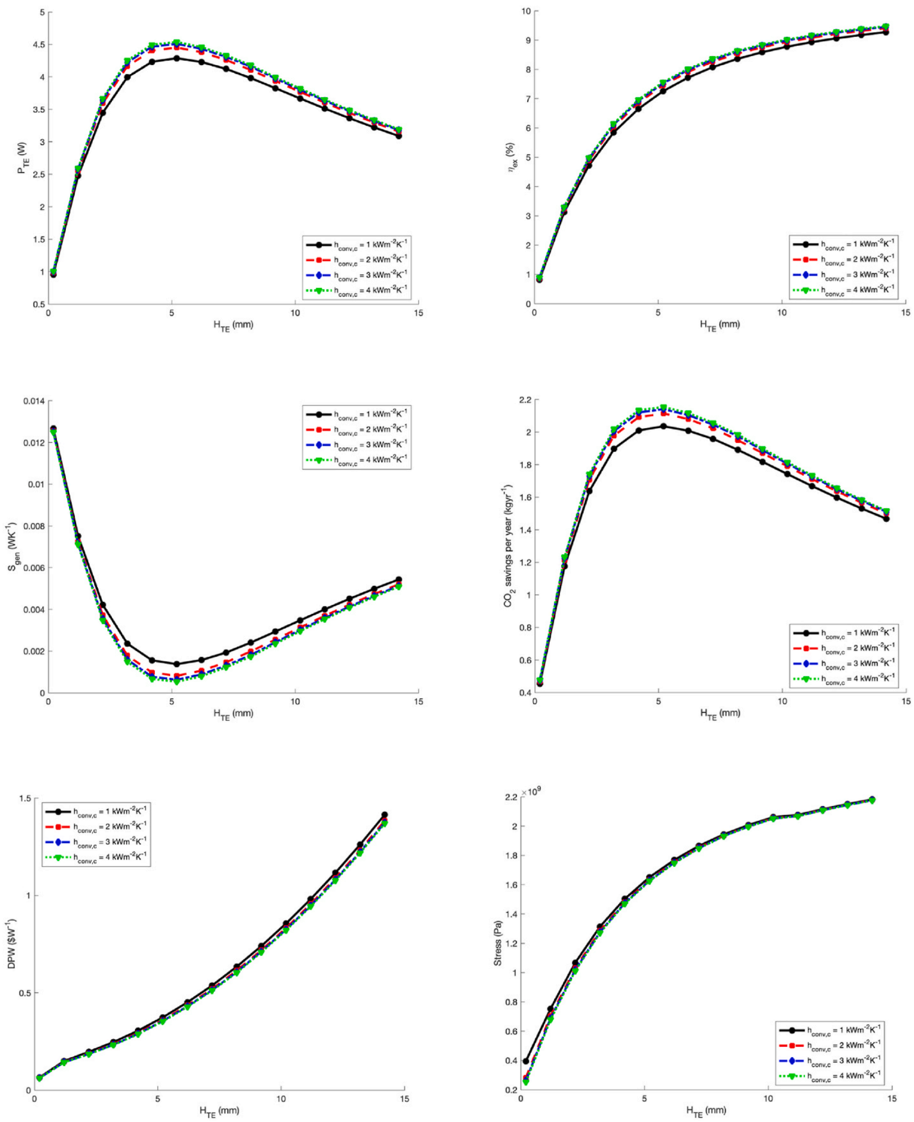

Fig. 3B. Effects of semiconductor height for various convective cooling film coefficients on power output, exergy efficiency, entropy generation, CO2 savings per year, dollars per watts, and thermal stress in the thermoelectric generator system.

savings. While higher semiconductor heights may offer advantages in terms of power output or thermal stress, they result in reduced CO_2 savings. This finding highlights the need to consider multiple factors and strike a balance between environmental considerations and other performance requirements during the design and optimization of the system. The dollars per watts ratio increased with increasing semiconductor height. The highest value of 1.41 $\$W^{-1}$ was achieved at a semiconductor height of 14.2 mm, while the lowest value of 0.06 $\$W^{-1}$ was observed at a semiconductor height of 0.2 mm for all convective cooling film coefficients. This suggests that higher semiconductor heights are associated with higher costs per unit of power output. Therefore, from an economic perspective, lower semiconductor heights may be more favorable as they result in a lower dollars per watts ratio, indicating better cost-effectiveness. The dollars per watts ratio is an important factor in determining the economic feasibility and market competitiveness of the thermoelectric generator system. Higher dollars per watts ratios may hinder the commercial viability of the technology, especially when compared to alternative energy generation methods. Therefore, optimizing the semiconductor height to achieve a favorable dollars per watts ratio is crucial for enhancing the economic attractiveness of the system. Thermal stress exhibited a positive correlation with semiconductor height. The highest thermal stress of 2.2 GPa occurred at a semiconductor height of 14.2 mm across all convective cooling film coefficients, while the lowest stress of 0.1 GPa was observed at a semiconductor height of 0.2 mm. Higher semiconductor heights led to increased thermal stress in the system.

The results from Fig. 3B demonstrate that the choice of semiconductor height in the thermoelectric generator system significantly influences power output, exergy efficiency, entropy generation, CO_2 savings, dollars per watts ratio, and thermal stress. Optimizing the semiconductor height is crucial to achieve the desired balance between these parameters, as higher heights lead to increased power output and exergy efficiency but also result in elevated entropy generation, reduced CO_2 savings, higher dollars per watts ratio, and greater thermal stress. Therefore, careful consideration of semiconductor height is essential to ensure an efficient, economically viable, and reliable thermoelectric generator system.

3.3. Semiconductor cross-sectional area

The cross-sectional area ratio of thermoelements is a crucial parameter in the design of thermoelectric energy conversion systems, with wide-ranging implications for the system's operational and economic performance as well as its environmental sustainability. To gain deeper insights into this, we conducted a detailed analysis, the results of which are presented and discussed in this section.

In our thermoelectric generator, changes in the cross-sectional area ratio directly impact the thermal and electrical characteristics of the system. Specifically, a larger cross-sectional area typically leads to higher heat dissipation, due to the increased area available for heat transfer. Conversely, a smaller cross-sectional area tends to retain more heat at the hot junction of the semiconductor, leading to a higher temperature gradient across the thermoelements.

This variation in heat dissipation and retention creates a distinct thermal distribution in the thermoelements, which sets the operating temperature of the semiconductor. The operating temperature, in turn, influences key semiconductor properties such as electrical resistivity, Seebeck coefficient, and thermal conductivity. These properties are integral to the energy conversion process, dictating the rate at which thermal energy is converted to electrical power.

Further, these changes in thermal and electrical properties reverberate through the performance of the thermoelectric generator, impacting its power output, exergy efficiency, and thermal stress levels. For instance, variations in thermal conductivity, driven by the change in the cross-sectional area ratio, modulate the temperature gradients across the thermoelements. These temperature gradients, coupled with changes in the electrical resistivity and Seebeck coefficient, subsequently affect the generator's power output and exergy efficiency.

Moreover, the choice of cross-sectional area ratio has a direct bearing on the system's dollar-per-watt metric and its CO_2 savings, critical indicators of its economic viability and environmental sustainability, respectively.

Given the intricate interplay between the cross-sectional area ratio and the system's performance parameters, it is vital to carefully select this ratio. Our analysis suggests that under standard operating conditions, an optimal balance between thermal conduction and electrical generation can lead to enhanced system performance. However, this balance is subject to the specific operating conditions, such as the concentrated solar heat flux, underscoring the need for further computational and experimental study for precise tailoring of the cross-sectional area ratio.

In conclusion, our analysis underscores the significance of the cross-sectional area ratio in the design and optimization of thermoelectric generators. By strategically selecting this parameter, one can effectively optimize the operational and economic performance of the system while also enhancing its environmental sustainability.

Fig. 4A shows that the power output exhibited a varying trend with respect to the semiconductor cross-sectional area (CSA) and concentrated solar irradiance. At the highest concentrated solar irradiance of 200 kWm^{-2}, the power output was maximum at 32.51 W with a CSA of

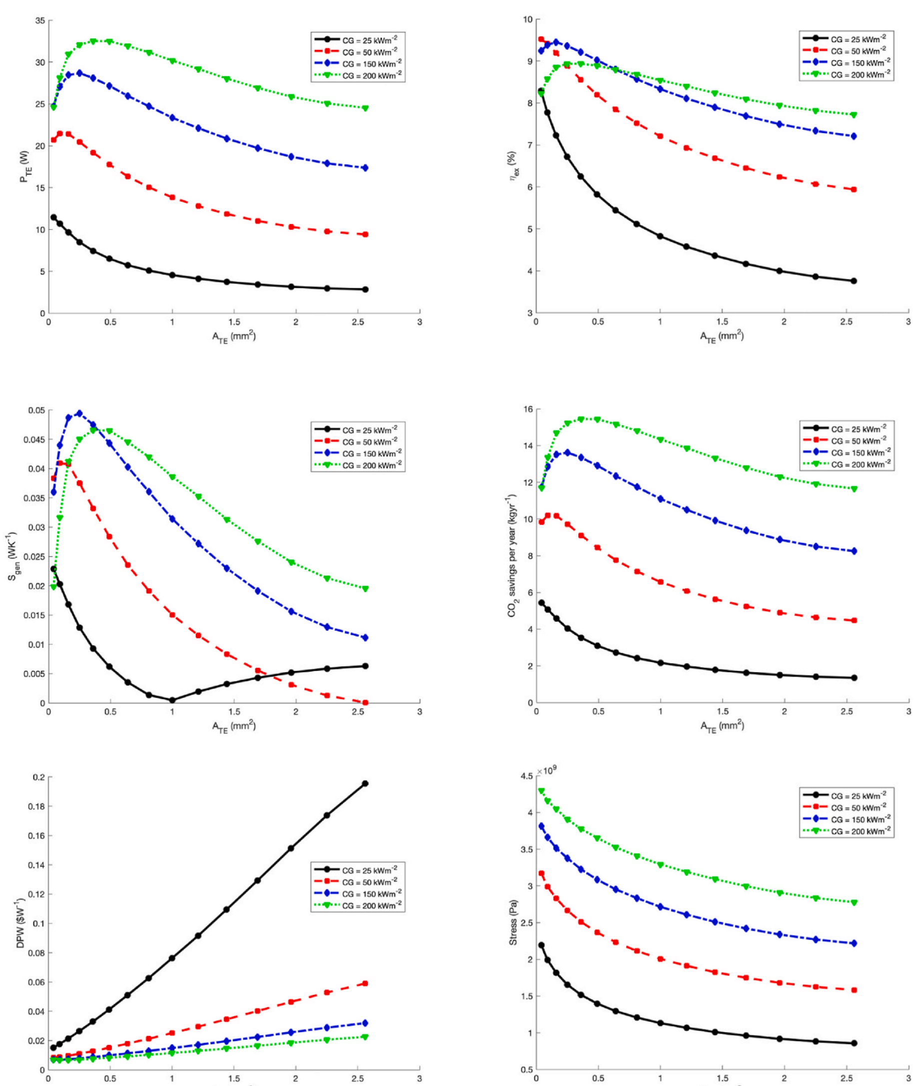

Fig. 4A. Effects of semiconductor cross-sectional area for various concentrated solar irradiance on power output, exergy efficiency, entropy generation, CO2 savings per year, dollars per watts, and thermal stress in the thermoelectric generator system.

0.36 mm^2, gradually decreasing to 24.54 W at 2.56 mm^2 CSA. Similarly, at the least concentrated solar irradiance of 25 kWm^{-2}, the power output peaked at 11.44 W with a CSA of 0.04 mm^2 and steadily decreased to 2.83 W at 2.56 mm^2 CSA. Decreasing the CSA generally led to an increase in power output, except for the lowest concentrated solar irradiance. The findings suggest that optimizing the CSA can enhance the power generation potential of the thermoelectric generator, especially at higher solar irradiances. Exergy efficiency exhibited varying patterns based on the CSA and solar irradiance. The highest efficiency of 9.52% was obtained at 0.04 mm^2 CSA for a concentrated irradiance of 50 kWm^{-2}, followed with a close-range exergy efficiency of 9.44% at 150 kWm^{-2} concentrated irradiance. The least exergy efficiencies were recorded at 2.56 mm^2 CSA for all irradiance levels. A maximum exergy efficiency of 8.28% was achieved at a concentrated solar irradiance of 25 kWm^{-2}, which decreased to the lowest value of 3.75% at 2.56 mm^2 CSA. The CSA and concentrated solar irradiance influenced the exergy efficiency of the system. Understanding the relationship between CSA, solar irradiance, and exergy efficiency can aid in designing and operating the generator for maximum energy conversion efficiency. Entropy generation demonstrated a fluctuating pattern across different concentrated solar irradiances. The maximum entropy generation occurred at a solar concentration irradiance of 150 kWm^{-2}, reaching 0.048 WK^{-1}, while the lowest value of 0.0004 WK^{-1} was obtained at 25 kWm^{-2} concentrated solar irradiance. Concentrated solar irradiances of 50 kWm^{-2} and 150 kWm^{-2} recorded entropy generations of 0.040 WK^{-1} and 0.048 WK^{-1}, respectively. The highest entropy generation was observed within the CSA range of 0.04–0.5 mm^2, and entropy decreased significantly at 2.5 mm^2 CSA for all solar irradiances. Managing and minimizing entropy generation can contribute to improving the overall performance and environmental sustainability of the thermoelectric generator. CO_2 savings per year exhibited variations based on the CSA and solar irradiance. The highest CO_2 saving per year was recorded at 200 kWm^{-2}, reaching 15.44 $kgyr^{-1}$ with a CSA of 0.36 mm^2, while the highest savings for the least solar irradiance of 25 kWm^{-2} was 5.43 $kgyr^{-1}$ at 0.04 mm^2 CSA. However, the maximum savings decreased to 11.65 $kgyr^{-1}$ at 2.56 mm^2 CSA for 200 kWm^{-2} concentrated irradiance, and for 25 kWm^{-2} irradiances, it dropped to 1.34 $kgyr^{-1}$ at 2.56 mm^2 CSA. CO_2 savings per year varied based on CSA and solar irradiance, with higher savings associated with smaller cross-sectional areas and higher solar irradiances. The section highlights the potential environmental benefits of the thermoelectric generator, emphasizing the importance of system optimization to maximize CO_2 reduction. The dollar per watt values indicated the economic aspect of the system. The highest value of 0.19 $\$W^{-1}$ was observed at a CSA of 2.56 mm^2 with a concentrating solar irradiance of 25 kWm^{-2}. In contrast, the least dollar per watt value for a concentrated solar irradiance of 200 kWm^{-2} was 0.022 $\$W^{-1}$ at 2.56 mm^2 CSA. The dollar per watt values varied with CSA and concentrating irradiance, reflecting the economic viability of power generation. Understanding the cost-effectiveness of the system under different conditions enables economic evaluations and decision-making regarding the deployment of the thermoelectric generator. Thermal stress experienced variations based on the concentrated solar irradiance and CSA. The maximum stress was observed at 200 KWm^{-2} concentrated solar irradiance, reaching 4.3 GPa with a CSA of 0.04 mm^2. At the least concentrated solar irradiance of 25 kWm^{-2}, the maximum stress recorded was 2.2 GPa at 0.04 mm^2 CSA. Thermal stress was influenced by solar irradiance and CSA, with varying maximum stress levels. Managing thermal stress is crucial for the durability and reliability of the system, and the results can inform the design and material selection to mitigate stress-related issues. In summary, the results showed that the semiconductor cross-sectional area and concentrated solar irradiance had significant effects on power output, exergy efficiency, entropy generation, CO_2 savings per year, dollar per watt values, and thermal stress. The findings provide insights into optimizing the performance of the concentrating solar segmented variable area leg thermoelectric generator in terms of energy, exergy, entropy, environmental impact, economic considerations, and thermo-mechanical aspects.

The results from Fig. 4A indicate that the choice of semiconductor cross-sectional area (CSA) and concentrated solar irradiance plays a crucial role in determining the performance of the thermoelectric generator system. Optimizing the CSA can enhance power output, exergy efficiency, and CO_2 savings, especially at higher solar irradiances. Understanding the relationship between CSA, solar irradiance, and exergy efficiency is essential for maximizing energy conversion efficiency. Managing and minimizing entropy generation can contribute to improved overall performance and environmental sustainability. The economic viability of the system is influenced by the CSA and solar irradiance, with higher savings associated with smaller cross-sectional areas and higher solar irradiances. Additionally, managing thermal stress is crucial for the durability and reliability of the system. These findings provide valuable insights into optimizing the system's performance in terms of energy, exergy, entropy, environmental impact, economic considerations, and thermo-mechanical aspects.

Fig. 4B expresses the variation of the system's power output. The plot indicates that the power output of the system is influenced by the semiconductor cross-sectional area and convective cooling film coefficients. The maximum power output of 11.81 W was achieved at a cross-sectional area of 0.04 mm^2, while the minimum power output of 2.94 W was observed at a cross-sectional area of 2.56 mm^2. The findings show that decreasing the cross-sectional area generally leads to higher power output, while increasing the cross-sectional area reduces the power output. This implies that optimizing the cross-sectional area can significantly impact the system's power generation capacity. The findings demonstrate that lower cross-sectional areas result in higher exergy efficiency, reaching up to 8.48%. Conversely, higher cross-sectional areas (2.56 mm^2) lead to lower exergy efficiency for all convective cooling film coefficients. These results suggest that smaller cross-sectional areas contribute to improved energy conversion efficiency, while larger cross-sectional areas decrease the system's overall exergy efficiency. The results show that the system experiences the least entropy generation (0.0004 WK^{-1}) at a cross-sectional area of 1 mm^2, which gradually increases to 0.006 WK^{-1} at a cross-sectional area of 2.56 mm^2 for all convective cooling film coefficients. Interestingly, the initial phase of the process with lower cross-sectional areas exhibits the highest entropy generation, reaching up to 0.024 WK^{-1} at 0.04 mm^2 and maintaining at that level the entropy generation at a cross-sectional area of 1.0 mm^2. These findings highlight the trade-off between cross-sectional area and entropy generation, indicating that larger areas contribute to increased energy losses and irreversibilities within the system. The result examines the impact of different cross-sectional areas and convective cooling film coefficients on CO_2 savings. The highest CO_2 savings per year, amounting to 5.63 $kgyr^{-1}$, was achieved at a cross-sectional area of 0.04 mm^2, irrespective of the convective cooling film coefficient applied. Conversely, the lowest CO_2 savings per year, totaling 1.34 $kgyr^{-1}$, was observed at a cross-sectional area of 2.56 mm^2 for all convective cooling film coefficients. These results indicate that reducing the cross-sectional area can significantly enhance the system's environmental performance by increasing CO_2 savings. The plot shows that higher cross-sectional areas, particularly at 2.56 mm^2, correspond to the highest dollars per watts ratio of 0.19 $\$W^{-1}$, while lower cross-sectional areas, specifically at 0.04 mm^2, result in the least dollars per watts ratio of 0.014 $\$W^{-1}$. This implies that increasing the cross-sectional area leads to higher costs per unit of power output, while reducing the cross-sectional area improves the economic feasibility of the system. Thermal stress refers to the mechanical stresses induced by temperature variations within the system. The results indicate that the maximum thermal stress of 2.19 GPa occurs at a cross-sectional area of 0.04 mm^2 for all convective cooling film coefficients, while the minimum stress of 0.79 GPa is observed at a cross-sectional area of 2.56 mm^2. These findings suggest that smaller cross-sectional areas subject the system to higher thermal stress, this could potentially affect the strength and longevity of

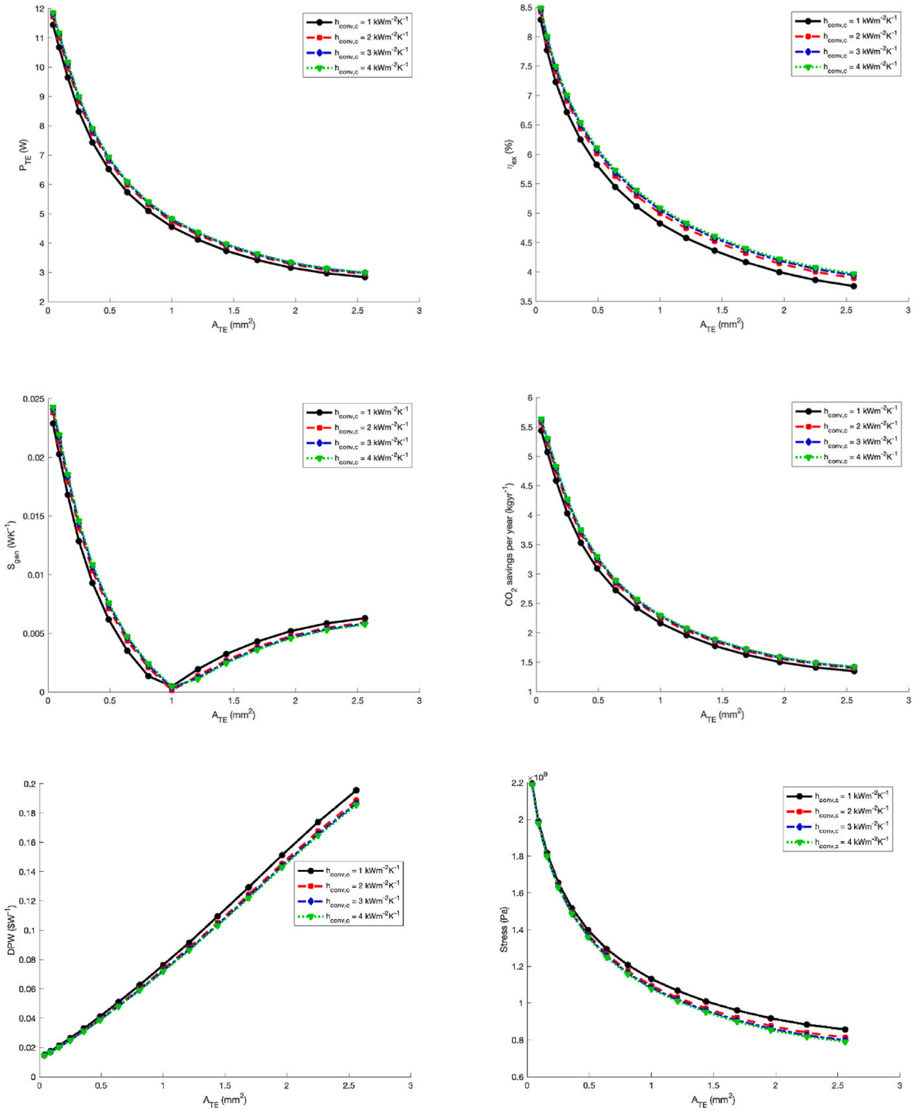

Fig. 4B. Effects of semiconductor cross-sectional area for various convective cooling film coefficients on power output, exergy efficiency, entropy generation, CO2 savings per year, dollars per watts, and thermal stress in the thermoelectric generator system.

the system's components. On the other hand, larger cross-sectional areas mitigate thermal stress, potentially improving the system's reliability. The comprehensive examination of the results reveals the relationship between the size of the semiconductor cross-sectional area and the convective cooling film coefficients, and their impact on the different performance aspects of the concentrating solar segmented variable area leg thermoelectric generator.

The results from Fig. 4B demonstrate the significant influence of the semiconductor CSA and convective cooling film coefficients on the performance of the thermoelectric generator system. Optimizing the CSA can enhance power output, exergy efficiency, and CO_2 savings, with smaller areas leading to higher efficiency and environmental benefits. However, the trade-off is observed with entropy generation, where smaller CSAs result in higher entropy production. The economic viability is also affected, with larger CSAs associated with higher dollars per watts ratios, impacting cost-effectiveness. Additionally, thermal stress is influenced by CSA, with smaller areas subjecting the system to higher stress levels. Overall, these findings provide crucial insights for system optimization, enhancing its performance, efficiency, and reliability in concentrated solar thermoelectric generator applications.

3.4. Amount of skutterudite

In this section, we delve into the nuanced impact of varying skutterudite (SKT) volume on the performance parameters of the concentrating solar segmented variable area leg thermoelectric generator. SKT and bismuth-telluride (BiTe) constitute the semiconductor materials used in our thermoelectric generator (TEG). SKT, known for its resilience at high temperatures, is contrasted with the low-temperature semiconductor, BiTe. Consequently, altering the SKT to BiTe volume ratio becomes a critical variable in enhancing the performance of our TEG. Through parametric analysis, we explored the ramifications of changing this ratio. A significant outcome of this change is the altered thermal distribution across the thermoelectric semiconductors, driven by the difference in thermal conductivities between SKT and BiTe. The variation in thermal distribution results in different temperature gradients between the hot and cold junctions of the TEG, thereby directly influencing the Seebeck voltage of the module. Changes in SKT to BiTe volume ratio also led to shifts in the electrical resistivities of these materials, thereby impacting the power output by modifying the electrical current flow and current densities within the semiconductor pellets. This modification results from the complex interaction of electrical resistivity, thermal conductivity, and Seebeck coefficients, which are all sensitive to changes in the SKT and BiTe volume ratio. The cascade effect of these changes profoundly impacts key performance parameters, such as exergy efficiency, CO_2 savings, and dollars per watts. These results underscore the importance of the SKT to BiTe volume ratio as a pivotal factor in optimizing the performance and viability of our novel TEG. Furthermore, the thermal stress levels within the device, a crucial aspect concerning the longevity and durability of our novel TEG, are also significantly influenced by changes in SKT volume. The varying thermal conductivities, which in turn alter the temperature distribution within the device, affect the thermal stress levels. In conclusion, our study highlights the significant role of SKT volume in determining the operational efficiency, financial viability, and durability of the novel TEG. Detailed analysis and results can be found in the subsequent paragraphs.

The results obtained from the analysis of the effects of the amount of skutterudite on the performance parameters of the concentrating solar segmented variable area leg thermoelectric generator are shown in Fig. 5A. The power output of the system was influenced by the amount of skutterudite and the concentrated solar irradiance. The amount of skutterudite and the concentrated solar irradiance had a significant impact on the power output of the system. Optimal power output was achieved at 6.17% skutterudite with a concentrated solar irradiance of 50 kWm^{-2}, resulting in a maximum power output of 47.47 W. However, as the skutterudite amount increased from this optimal value, the power output decreased. The findings suggest that the amount of skutterudite plays a crucial role in determining the power generation capability of the system and the importance of skutterudite composition in achieving optimal system performance. The exergy efficiency shows that the system consistently experienced its lowest exergy efficiency for all concentrated solar irradiance levels at 92.5% skutterudite amount. This finding suggests that an optimal skutterudite content is around 6.17%, where the exergy efficiency is maximized. This indicates that an excessive amount of skutterudite negatively impacts the exergy conversion efficiency of the system. It highlights the importance of avoiding an overabundance of skutterudite, as it can lead to diminishing returns and reduced overall system performance. By finding the right balance between skutterudite amount and solar irradiance, it is possible to achieve higher exergy efficiency and, consequently, improve the system's exergy conversion capabilities. The system exhibited a complex pattern of entropy generation, with both increasing and decreasing trends observed across the skutterudite range. The highest entropy generation of 0.129 WK^{-1} was observed at 6.17% skutterudite and a concentrated solar irradiance of 50 kWm^{-2}, while the least entropy generation of 0.0007 WK^{-1} occurred at 37.03% skutterudite with a concentrated solar irradiance of 25 kWm^{-2}. Managing entropy generation is crucial for

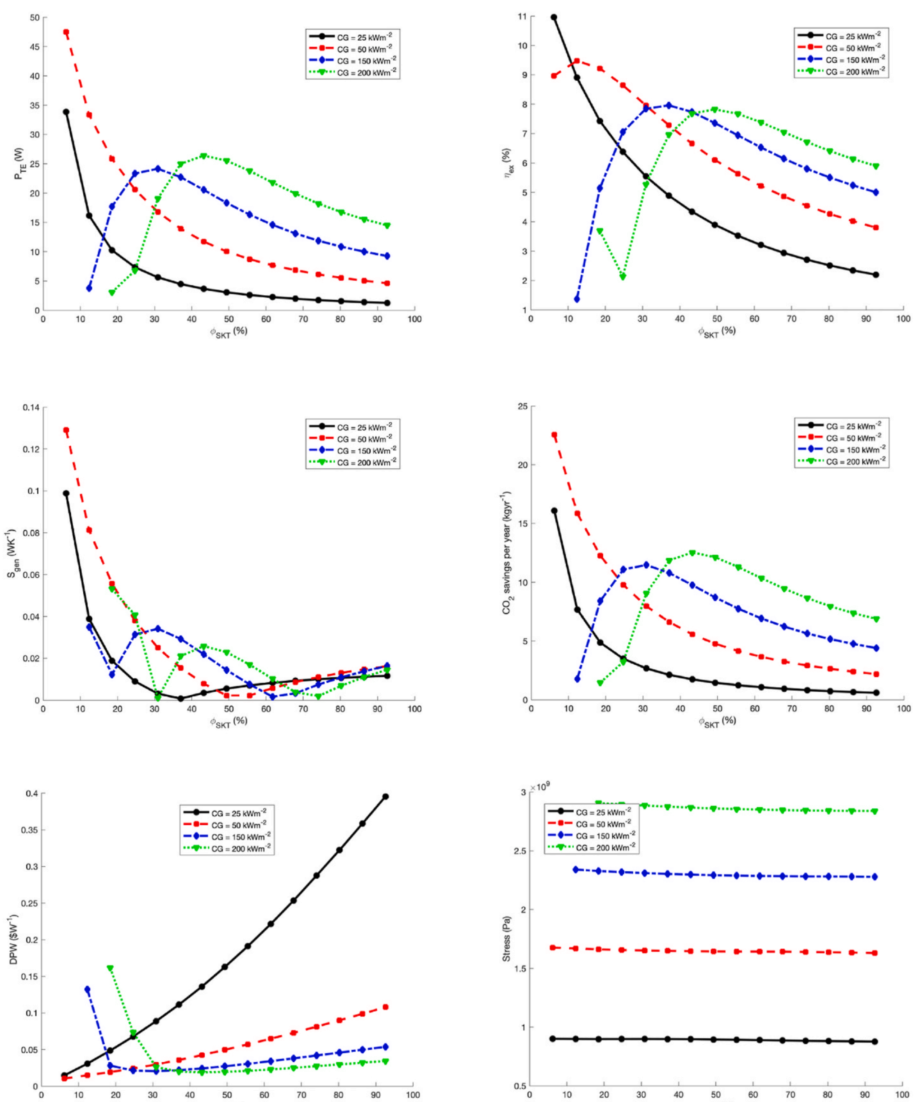

Fig. 5A. Effects of skutterudite amount for various concentrated solar irradiance on power output, exergy efficiency, entropy generation, CO2 savings per year, dollars per watts, and thermal stress in the thermoelectric generator system.

improving the overall performance and efficiency of the thermoelectric generator. The results highlight the influence of skutterudite amount on entropy generation. Maximum CO_2 savings of 22.55 $kgyr^{-1}$ were achieved at 6.17% skutterudite with a concentrated solar irradiance of 50 kWm^{-2}. The lowest savings of 0.59 $kgyr^{-1}$ occurred at 92.5% skutterudite with a concentrated solar irradiance of 25 kWm^{-2}. These findings demonstrate the potential of the system to contribute to environmental sustainability by reducing CO_2 emissions. Optimizing the skutterudite amount can contribute to maximizing the environmental benefits of the system by reducing CO_2 emissions. The results emphasize the importance of considering skutterudite composition for sustainable energy production. The dollars per watts values varied with different skutterudite amounts and concentrated solar irradiance levels. While the system couldn't achieve up to 0.2 $\$W^{-1}$ for concentrated solar irradiance levels of 50 kWm^{-2} and above, it reached a maximum value of 0.39 $\$W^{-1}$ at 92.5% skutterudite with a concentrated solar irradiance of 25 kWm^{-2}. Optimizing the skutterudite amount can influence the cost-effectiveness of power generation. The findings provide insights for economic evaluations and decision-making regarding the implementation of the thermoelectric generator. The results indicate a direct correlation between the level of concentrating solar irradiance and the stress experienced by the system. As the solar irradiance increased, the stress levels also increased. The maximum stress observed was 2.89 GPa at a concentrating solar irradiance of 200 kWm^{-2}, while the stress decreased to 2.34 GPa, 1.68 GPa, and 0.87 GPa for 150 kWm^{-2}, 50 kWm^{-2}, and 25 kWm^{-2}, respectively. The stress levels experienced by the system are essential indicators of its structural integrity and mechanical performance. Higher stress levels can potentially lead to material deformation, component failure, or reduced lifespan of the system. Therefore, it is crucial to consider the stress levels and their effects when designing and operating the concentrating solar segmented variable area leg thermoelectric generator.

The results from Fig. 5A highlight the critical role of skutterudite amount and concentrated solar irradiance in determining the performance of the thermoelectric generator system. Managing skutterudite composition is crucial for achieving high energy conversion efficiency and overall system performance. The complex pattern of entropy generation emphasizes the need to carefully control skutterudite amount to minimize energy losses and system inefficiencies. Moreover, optimizing skutterudite content enables significant CO_2 savings, enhancing the environmental sustainability of the system. Additionally, the study demonstrates the influence of concentrated solar irradiance on thermal stress, with higher irradiance levels leading to increased stress. Managing stress levels is essential to ensure the system's structural integrity

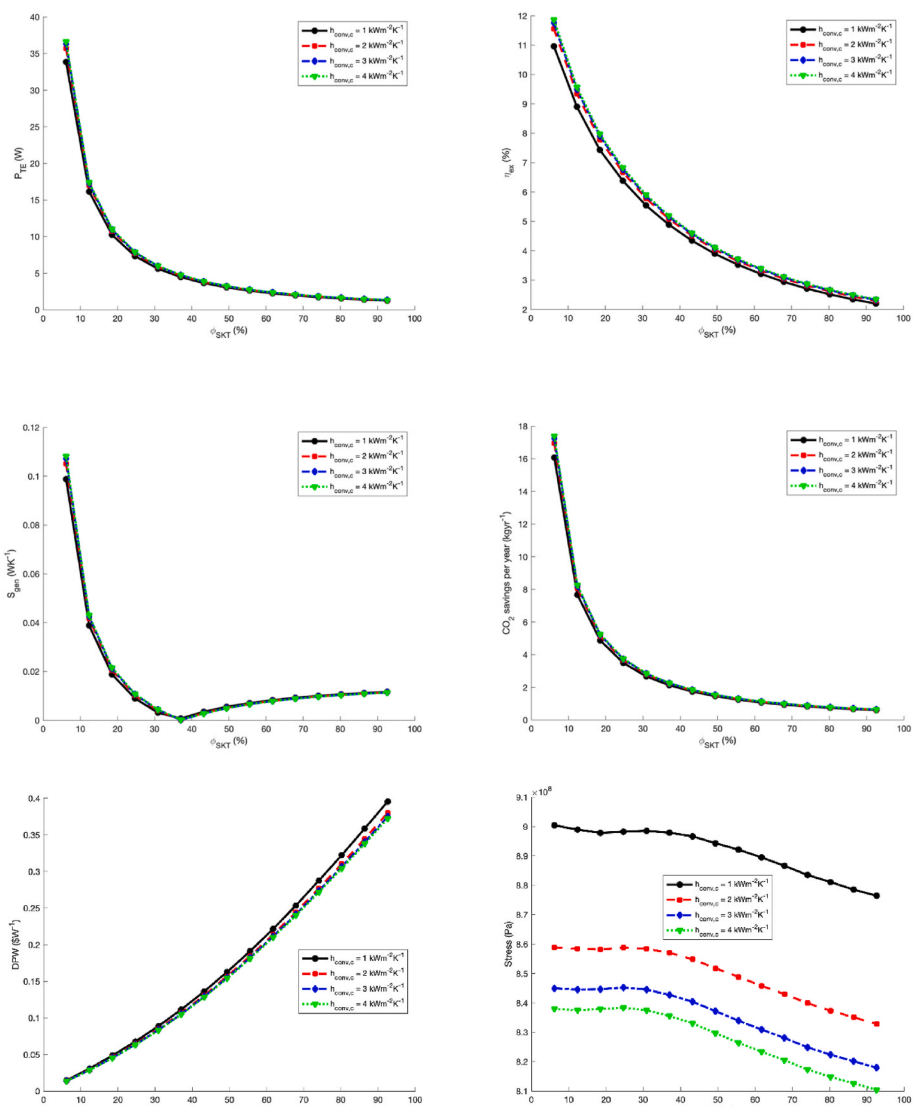

Fig. 5B. Effects of skutterudite amount for various convective cooling film coefficients on power output, exergy efficiency, entropy generation, CO2 savings per year, dollars per watts, and thermal stress in the thermoelectric generator system.

and longevity. Overall, the results provide valuable insights for the design and optimization of the thermoelectric generator system, with implications for power generation efficiency, environmental impact, and system reliability.

Fig. 5B shows the variation of the system's power output. The power output showed a significant increase at lower skutterudite content of 6.17% with an optimal power output of 35.6 W. However, the power output decreased to 1.26 W at higher skutterudite amount of 92.5% across all convective cooling film coefficients. Higher skutterudite content resulted in lower power output. The exergy efficiency demonstrated a consistent behavior across all convective cooling film coefficients. The optimal exergy efficiency of 11.86% was achieved at 6.17% skutterudite amount, while the minimum efficiency of 2.19% was observed at 92.5% skutterudite amount. Higher skutterudite amount led to decreased exergy efficiency. The entropy generation varied with skutterudite content. The maximum entropy generation of 0.10 WK^{-1} occurred at 6.17% skutterudite content, while at 35% skutterudite amount, the entropy generation dropped to 9×10^{-5} WK^{-1}. At 92.5% amount of skutterudite content, there was a slight increase in entropy generation to 0.011 WK^{-1}. Higher skutterudite content correlated with lower entropy generation even with varying convective cooling film coefficient. The system achieved the highest CO_2 savings per year of approximately 17.39 $kgyr^{-1}$ at 6.17% skutterudite content across all convective cooling film coefficients. Conversely, the lowest CO_2 savings per year of 0.59 $kgyr^{-1}$ occurred at 92.5% skutterudite content. Higher skutterudite content resulted in reduced CO_2 savings when higher skutterudite amount is applied across all convective cooling film coefficient. The convective cooling film coefficient of 1 $kWm^{-2}K^{-1}$ yielded the highest dollars per watts of 0.39 $\$W^{-1}$ at 92.5% skutterudite content, slightly higher than the convective cooling film coefficients of 2, 3, and 4 $kWm^{-2}K^{-1}$. The lowest dollars per watts of 0.013 $\$W^{-1}$ was observed at 6.17% skutterudite content for all convective cooling film coefficients. The system experienced the highest thermal stress of 0.9 GPa at 6.17% skutterudite content with a 1 kWm^{-2} K^{-1} convective cooling film coefficient. The least thermal stress of 0.81 GPa was observed at 92.5% skutterudite content with a 4 kWm^{-2} K^{-1} convective cooling film coefficient. The results indicate that the skutterudite content and convective cooling film coefficients have a significant impact on the performance parameters of the thermoelectric generator. Higher skutterudite content generally led to decreased power output, exergy efficiency, and CO_2 savings per year, but increased entropy generation and thermal stress. The convective cooling film coefficients influenced the dollars per watts ratio.

The study investigated the impact of skutterudite content on various performance parameters of the concentrating solar segmented variable area leg thermoelectric generator (CSSTEG). Fig. 5A and B provided graphical representations illustrating the relationship between skutterudite content and performance parameters. The optimal power output of 47.47 W was achieved at a skutterudite content of 6.17% and a solar irradiance of 50 kWm^{-2}, while deviations from this composition resulted in declining power output. Similarly, exergy efficiency was significantly influenced by skutterudite content, with the highest efficiency of 11.86% attained at 6.17% skutterudite content. Higher or lower proportions led to decreased exergy efficiency. The impact of skutterudite content on entropy generation was also evident, with an optimal composition of 6.17% yielding the highest entropy generation, while deviations resulted in reduced entropy generation. Furthermore, the amount of skutterudite influenced the CO_2 savings per year, with 22.55 $kgyr^{-1}$ achieved at 6.17% skutterudite content and 50 kWm^{-2} solar irradiance. At 92.5% skutterudite content and 25 kWm^{-2} solar irradiance, CO_2 savings reduced to 0.59 $kgyr^{-1}$. The dollars per watts values were affected by skutterudite content as well, with the peak value of 0.39 $\$W^{-1}$ obtained at 92.5% skutterudite content and 25 kWm^{-2} solar irradiance. In contrast, at higher irradiance levels, the system fell short of the target value. Finally, the thermal stress experienced by the generator was closely related to skutterudite content, with higher content and solar irradiance leading to increased stress levels, emphasizing the importance of optimizing skutterudite composition for structural integrity.

These results highlight the critical role/impact of skutterudite content in influencing the performance and efficiency of the CSSTEG. Achieving an optimal skutterudite composition is vital to maximize power output, exergy efficiency, CO_2 savings, dollars per watts, and manage thermal stress effectively.

3.5. Semiconductor cross-sectional area ratio

Fig. 6A shows the effects of the area ratio on the power output at different solar fluxes. The power output of the system varied with changes in the semiconductor cross-sectional area ratio. The highest power output of 27.19 W was achieved at a concentrated solar irradiance of 200 kWm^{-2} and a low cross-sectional area ratio of 3.06. However, the power output decreased to 3.84 W at a cross-sectional area ratio of 49 with a concentrated solar irradiance of 25 kWm^{-2}. This suggests that optimizing the cross-sectional area (CSA) ratio can significantly impact the power generation capacity of the system. The exergy efficiency of the system decreased as the semiconductor cross-sectional area ratio increased. The maximum exergy efficiency of 7.98% was obtained at a concentrated solar irradiance of 200 kWm^{-2} and a cross-sectional area ratio of 0.76. This indicates that the choice of cross-sectional area ratio can influence the overall efficiency of the system in converting input energy into useful work. The study revealed that entropy generation varied with changes in the semiconductor cross-sectional area ratio. Initially, there was a slight increase in entropy generation in the 0.7–5.4 CSA ratio range for a concentrated solar irradiance of 200 kWm^{-2}. The maximum entropy generation of 0.028 WK^{-1} occurred at the same concentrated solar irradiance. However, as the CSA ratio increased, entropy generation decreased significantly, reaching its minimum value of 0.004 WK^{-1} at a CSA ratio of 49. This demonstrates the influence of the CSA ratio on the system's ability to minimize energy losses and maximize performance efficiency. The CO_2 savings per year were influenced by both the CSA ratio and the concentrated solar irradiance. The highest CO_2 savings of 12.91 $kgyr^{-1}$ were achieved at a CSA ratio of 3.06 and a concentrated solar irradiance of 200 kWm^{-2}. On the other hand, the minimum CO_2 savings of 1.43 $kgyr^{-1}$ occurred at a CSA ratio of 49 and a concentrated solar irradiance of 200 kWm^{-2}. The effect of CO_2 savings per year findings demonstrates that selecting an optimal cross-sectional area ratio can lead to significant annual CO_2 emissions reductions, highlighting the environmental benefits of system optimization. The dollars per watts metric provides insights into the economic efficiency of the system. In this study, the dollar per watts value varied with changes in both the CSA ratio and the concentrated solar irradiance. With a concentrated solar irradiance of 25 kWm^{-2}, the system achieved its highest dollars per watts value of 0.17 $\$W^{-1}$ at a CSA ratio of 0.76, which gradually decreased to 0.08 $\$W^{-1}$ at 21.77 CSA ratio. As the CSA ratio increased, the dollars per watts value decreased further, reaching its minimum of 0.013 $\$W^{-1}$ at a CSA ratio of 49. These findings indicate that the choice of CSA ratio can have economic implications, impacting the cost-effectiveness of the system. The results demonstrate that the thermal stress experienced by the system varied with changes in the CSA ratio and the concentrated solar irradiance. The maximum thermal stress of 3.47 GPa occurred at a CSA ratio of 49 and a concentrated solar irradiance of 200 KWm^{-2}, while the minimum thermal stress of 0.88 GPa was observed at 0.76 semiconductor cross sectional area ratio with a concentrated solar irradiance of 25 kWm^{-2}. The effect of thermal stress findings indicates that higher cross-sectional area ratios result in increased thermal stress levels, which may have implications for the structural integrity and durability of the system components, requiring careful consideration in design and operation.

The findings from Fig. 6A highlight the significant impact of the semiconductor cross-sectional area ratio on the thermoelectric

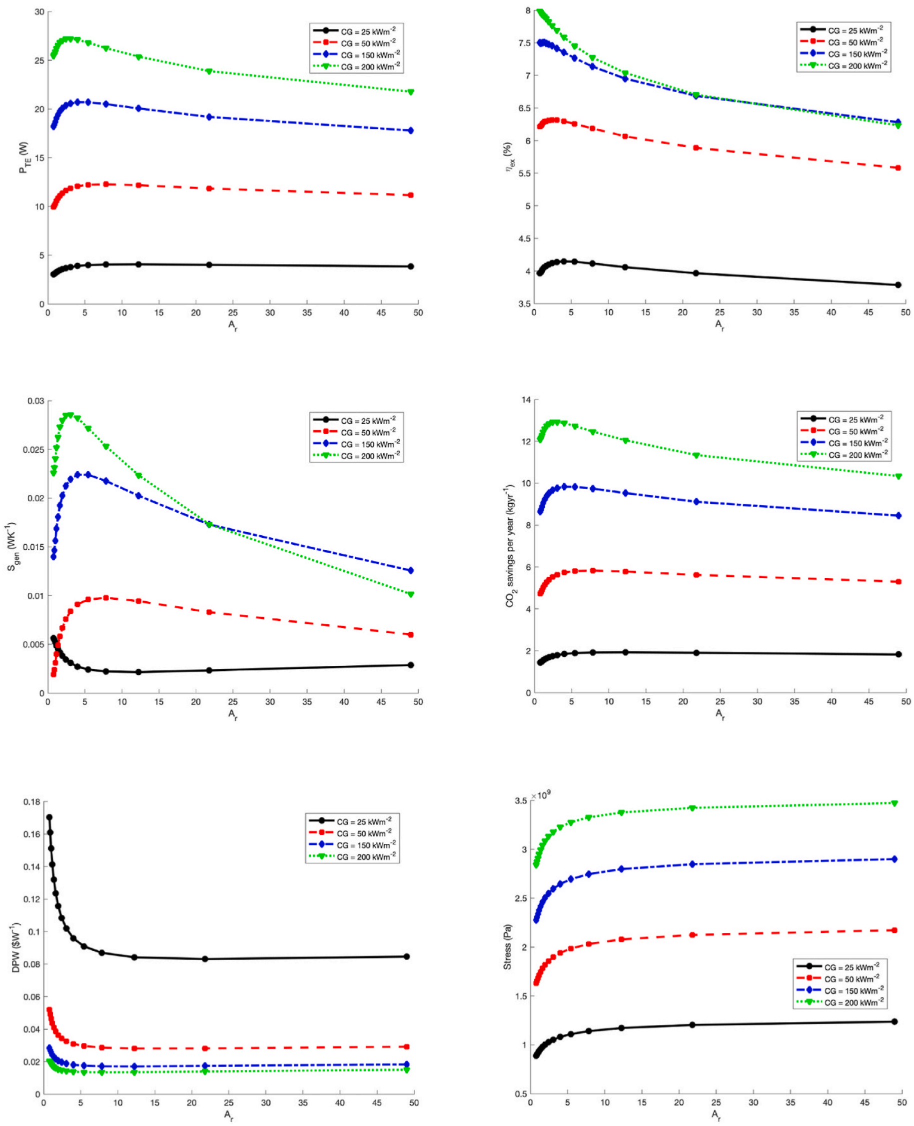

Fig. 6A. Effects of semiconductor cross-sectional area ratio for various concentrated solar irradiance on power output, exergy efficiency, entropy generation, CO2 savings per year, dollars per watts, and thermal stress in the thermoelectric generator system.

generator system's performance. Optimizing the area ratio can lead to substantial improvements in power output, exergy efficiency, and CO_2 savings, while minimizing entropy generation and thermal stress. Additionally, the economic viability of the system is influenced by the choice of area ratio, with lower ratios leading to higher cost-effectiveness. Understanding and carefully selecting the appropriate cross-sectional area ratio can enhance the system's overall efficiency, environmental sustainability, and economic attractiveness, crucial for successful deployment and operation.

Fig. 6B shows that the power output of the system exhibited a clear trend with respect to the semiconductor cross-sectional area ratio and convective cooling film coefficients. The highest power output was observed within the range of 0.76–25 cross-sectional area ratio for all convective cooling coefficients, with a peak value of 4.32 W. However, as the cross-sectional area ratio increased to 49, the power output significantly decreased to 1.81 W for all convective cooling film coefficients. This indicates that decreasing the cross-sectional area ratio is crucial for maximizing power generation in the system. Exergy efficiency is an important measure of the system's ability to convert available energy into useful work. The findings revealed that the exergy efficiency decreased as the cross-sectional area ratio increased. The maximum exergy efficiency of 4.38% was achieved at the lowest cross-sectional area ratio of 4.0 with a convective cooling film coefficient of 4 kWm^{-2} K^{-1}. Conversely, the lowest exergy efficiency of 2.74% was observed at the highest cross-sectional area ratio of 49 with a convective cooling coefficient of 1 kWm^{-2} K^{-1}. These results indicate that a smaller cross-sectional area ratio enhances the system's energy conversion efficiency with a higher convective cooling film coefficient. Entropy generation represents the measure of irreversibility and energy losses within the system. The findings demonstrated that increasing the semiconductor cross-sectional area ratio led to higher entropy generation. The maximum entropy generation of 0.0097 WK^{-1} was observed at 49 cross-sectional area ratios with a convective cooling film coefficient of 1 kWm^{-2} K^{-1}, while the minimum entropy generation of 0.0012 WK^{-1} occurred at a cross-sectional area ratio of 12.25 with a convective cooling coefficient of 4 kWm^{-2} K^{-1}. These results suggest that larger cross-sectional area ratios contribute to increased energy losses and reduced system efficiency when lower convective cooling film coefficient is applied. The study investigated the CO_2 savings achieved by the system based on different cross-sectional area ratios and convective cooling film coefficients. The results revealed that the system attained the highest CO_2 savings per year of 2.05 $kgyr^{-1}$ at a cross-sectional area

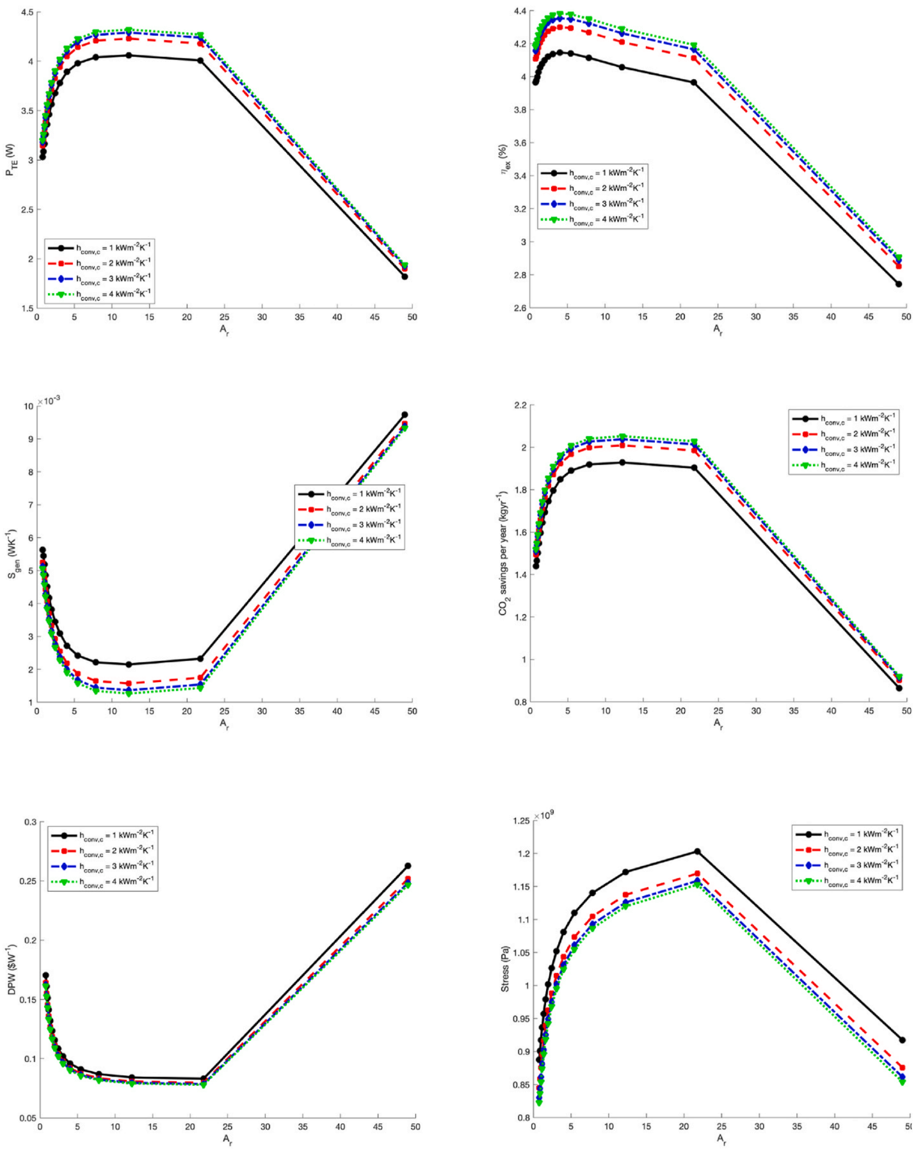

Fig. 6B. Effects of semiconductor cross-sectional area ratio for various convective cooling film coefficients on power output, exergy efficiency, entropy generation, CO2 savings per year, dollars per watts, and thermal stress in the thermoelectric generator system.

ratio of 12.25 for both 3 kWm^{-2} K^{-1} and 4 kWm^{-2} K^{-1} convective cooling film coefficients. However, as the cross-sectional area ratio increased to 49, the CO_2 savings per year drastically decreased to 0.86 $kgyr^{-1}$. These findings emphasize the significance of selecting an optimal cross-sectional area ratio to maximize the environmental benefits of the system. The economic viability of the system was assessed using the dollars per watts metric. The findings indicated that the dollars per watts value increased with larger cross-sectional area ratios. At a cross-sectional area ratio of 49, the system recorded a dollars per watts value of 0.26 $\$W^{-1}$ for a convective cooling film coefficient of 1 kWm^{-2} K^{-1}, and 0.25 $\$W^{-1}$ for convective cooling film coefficients of 2 kWm^{-2} K^{-1}, 3 kWm^{-2} K^{-1}, and 4 kWm^{-2} K^{-1}. These results suggest that larger cross-sectional area ratios may lead to higher economic costs for power generation, highlighting the need for optimizing the cross-sectional area ratio to ensure cost-effective system operation. The thermal stress experienced by the system was examined in relation to different cross-sectional area ratios and convective cooling film coefficients. The results showed that the thermal stress gradually increased from low to moderate values and then decreased as the cross-sectional area ratio increased to 49. For the convective cooling film coefficients investigated, the thermal stress ranged from 0.85 GPa to 0.88 GPa at a cross-sectional area ratio of 49. These findings indicate that the choice of cross-sectional area ratio influences the distribution of thermal stress within the system, with implications for structural integrity and durability.

3.5.1. Semi-conductor cross sectional area optimization insights

For power output, an optimal cross-sectional area ratio of 3.06 yielded the highest power output of 27.19 W at a concentrated solar irradiance of 200 kWm^{-2}. Conversely, a cross-sectional area ratio of 49 resulted in a reduced power output of 3.84 W at a solar irradiance of 25 kWm^{-2}. This highlights the critical importance of optimizing the cross-sectional area ratio to maximize power generation capacity. Regarding exergy efficiency, a smaller cross-sectional area ratio of 0.76 exhibited the highest efficiency of 7.98% at a solar irradiance of 200 kWm^{-2}. In contrast, the highest cross-sectional area ratio of 49 resulted in a lower exergy efficiency of 2.74%. This emphasizes the significance of selecting an appropriate cross-sectional area ratio to enhance energy conversion efficiency. Entropy generation was also affected by the cross-sectional area ratio, with the lowest entropy generation of 0.004 WK^{-1} observed at a ratio of 49. A smaller cross-sectional area ratio, within the range of 0.7–5.4, appeared to reduce entropy generation, indicating a more favorable thermodynamic performance. The choice of cross-sectional area ratio further influenced the CO_2 savings, with the highest savings of 12.91 $kgyr^{-1}$ achieved at a ratio of 3.06 and a solar irradiance of 200 kWm^{-2}. A lower cross-sectional area ratio, in this case, promoted higher CO_2 savings, demonstrating the environmental benefits of system optimization. Economic efficiency, as measured by the dollars per watts metric, also varied with the cross-sectional area ratio. Larger ratios resulted in higher values, indicating potential increased costs for power generation. To ensure cost-effective system operation, optimization of the cross-sectional area ratio is necessary. Finally, thermal stress distribution was influenced by the cross-sectional area ratio, with lower ratios resulting in lower thermal stress levels. This is crucial for maintaining the structural integrity and durability of the system.

Based on our findings, we recommend selecting a cross-sectional area ratio within the range of 0.7–5.4 for a concentrated solar irradiance of 200 kWm^{-2} to achieve optimal performance in power output, exergy efficiency, entropy generation, CO_2 savings, and thermal stress. This range strikes the best balance between power generation capacity, energy conversion efficiency, environmental sustainability, and economic viability, contributing to the development of high-performance and durable TEGs.

3.6. Overall optimization insights – enviro-economic metrics

The environmental and economic outcomes of our thermoelectric generator (TEG) system are intrinsically tied to its design parameters—namely the skutterudite (SKT) content, the cross-sectional area ratio of the thermoelectric elements, and the level of concentrated solar irradiance.

Starting with SKT content, its manipulation greatly influences the system's thermoelectric performance due to SKT's status as a high-temperature thermoelectric material. A higher SKT content alters the thermal distribution within the semiconductor pellets, increasing the operating temperature and thereby enhancing the thermoelectric characteristics of the system. This primarily includes the Seebeck coefficient, electrical resistivity, and thermal conductivity—all key determinants of the system's efficiency and power output.

The cross-sectional area ratio of the thermoelectric elements functions similarly. By adjusting this ratio, we change the heat retention capacity at the hot junction of the TEG. Smaller cross-sectional areas lead to higher heat retention and thus higher operating temperatures, once again optimizing the thermoelectric performance.

The concentrated solar irradiance level, acting as the primary heat source for the TEG system, also directly affects the operating temperature. Higher irradiance levels lead to more heat absorption, increasing the operating temperature and enhancing the system's thermoelectric efficiency.

The environmental implications of these parameters are significant. More efficient TEG operation leads to higher power outputs and therefore greater CO2 savings, as the renewable energy generated decreases reliance on fossil fuels. This has the dual benefit of lowering greenhouse gas emissions while contributing to energy sustainability.

In economic terms, the parameters' effects are equally profound. Higher power output increases potential revenue from energy generation, while higher device efficiency decreases operational costs over the device's lifecycle.

In conclusion, the interplay between SKT content, cross-sectional area ratios, and concentrated solar irradiance levels necessitates thoughtful calibration to achieve optimal environmental and economic outcomes.

3.7. Practical applications and implications

The practicality of our research goes beyond mere theoretical exploration; it provides concrete, applicable solutions to enhance energy efficiency across diverse sectors. Our study has significant implications in environments where waste heat is generated as a by-product, such as power plants, industrial processes, and automotive systems. The implementation of our optimized segmented thermoelectric generator (TEG) system facilitates the efficient transformation of this waste heat into reusable electrical energy, thereby augmenting overall energy efficiency and playing a vital role in CO_2 emissions reduction, an essential aspect in combating climate change.

Our system, constituted by segmented materials, exhibits superiority over traditional single-material TEGs by offering a broader temperature operating range. This particular attribute opens doors for various industrial applications, particularly in industries like steel and glass manufacturing, where waste heat temperatures vary greatly.

The practical implications of our research extend to the realm of renewable energy. Our study provides an effective solution for transforming concentrated solar irradiance into electricity, a timely contribution as the world shifts its focus towards more sustainable and renewable energy sources. Our TEG system could play a pivotal role in harnessing the vast yet largely underutilized energy potential of the sun.

In remote or off-grid locations, as well as emergency situations where access to conventional power sources might be constrained, our high-efficiency segmented TEG system offers a reliable, independent power solution. By harnessing waste heat or solar energy, our system can supply indispensable electricity for communication devices, medical equipment, or other essential utilities, demonstrating its instrumental value in such scenarios.

The insights drawn from our research provide a roadmap to enhance energy efficiency across numerous systems, aligning with the broader global goal of sustainable development. We eagerly anticipate the practical implementations of our high-efficiency segmented TEG system in these and other related applications, highlighting the real-world utility of our theoretical findings.

4. Conclusions

In conclusion, the comprehensive analysis conducted in this study on the energy, exergy, entropy, environmental, economic, and thermo-mechanical performance optimization of a concentrating solar segmented variable area leg thermoelectric generator provides valuable insights into the design and operation of efficient and sustainable energy systems. The findings demonstrate the complex interplay between various parameters such as semiconductor geometry (height, area, and area ratio), amount of skutterudite, convective cooling film coefficients, concentrated solar irradiance, and their impacts on key performance indicators of the system which include the power output, exergy efficiency, entropy generation, dollar per watts, and thermal stress. Based on the results discussed, the ensuing conclusions are made:

1. Generally, the power generation, CO_2 savings and most times the exergy efficiency attained the highest possible optimal value when the concentrated solar irradiance was varied for a fixed heat transfer coefficient. On the other hand, the thermal stress and dollar per watt were minimized when the convective heat transfer coefficient was varied and the concentrated solar flux was held constant.
2. Of all the parameters studied in this work, it was found that the Skutterudite content exerted the highest impact on the power generation, exergy efficiency and CO_2 savings of the systems. The system generated the maximum power of 47.47 W as well as CO_2 savings of 22.5 $kgyr^{-1}$ at an optimum skutterudite amount of 6.17% when operated under a fixed solar irradiance of 50 kWm^{-2}. Meanwhile, at these conditions, the system's exergy efficiency attained its maximum value of 10.95% at a lower flux of 25 kWm^{-2} for the same amount of skutterudite.
3. Optimization of the semiconductor height in the design had a significant impact on both thermal stress and cost. The findings indicate that selecting a semiconductor height of 0.2 mm led to the least

overall thermal stress of 0.25 GPa at 4 $kWm^{-2}K^{-1}$ cooling heat transfer coefficient and the least overall cost per watt of 0.0048 $\$W^{-1}$ at 100 kWm^{-2} concentrated solar irradiance. These results highlight the importance of semiconductor height in improving the system's thermo-mechanical performance, and economic feasibility.

The results highlight the importance of considering trade-offs and selecting optimal values for the semiconductor cross-sectional area and convective cooling film coefficients to achieve desired system performance. Lower cross-sectional areas generally lead to higher power output and exergy efficiency, while higher cross-sectional areas result in increased thermal stress. The convective cooling film coefficients play a crucial role in determining exergy efficiency, entropy generation, CO_2 savings, and dollar per watt efficiency. By optimizing these parameters, it is possible to enhance the energy conversion efficiency, minimize entropy generation, reduce CO_2 emissions, and improve the economic viability of the system. Furthermore, the study emphasizes the need to ensure the structural integrity and durability of the components, as thermal stress can impact the long-term performance of the system. This research contributes to advancing the field of concentrating solar thermoelectric technology by providing valuable insights for system optimization. The findings have practical implications for the design and implementation of efficient and sustainable energy generation systems, ultimately contributing to the development of a cleaner and more sustainable future. Future research will intend to investigate the optimal design and integration into hybrid systems, multi-objective optimization, advanced cooling techniques, and operation under real world conditions.

CRediT authorship contribution statement

Hisham Alghamdi: Methodology, Software, Validation, Formal analysis, Investigation, Writing – original draft, Writing – review & editing, Visualization. **Chika Maduabuchi:** Conceptualization, Methodology, Software, Validation, Formal analysis, Investigation, Resources, Data curation, Writing – original draft, Writing – review & editing, Visualization, Supervision, Project administration. **Kingsley Okoli:** Methodology, Resources, Data curation, Writing – review & editing, Supervision, Project administration. **Abdullah Albaker:** Methodology, Software, Validation, Formal analysis, Investigation, Resources. **Ibrahim Alatawi:** Investigation, Resources, Data curation, Writing – review & editing. **Mohammed Alghassab:** Supervision, Project administration, Funding acquisition. **Hind Albalawi:** Software, Validation, Formal analysis, Investigation. **Mohammad Alkhedher:** Methodology, Resources, Data curation, Writing – review & editing.

Declaration of competing interest

The authors declare that they have no known competing financial interests or personal relationships that could have appeared to influence the work reported in this paper

Data availability

The authors do not have permission to share data.

Acknowledgements

The authors would like to thank the The Deanship of Scientific Research at Najran University for funding this work under the grant code (NU/DRP/SERC/12/12), the Deanship of Scientific Research at Shaqra University for supporting this work, the Princess Nourah bint Abdulrahman University Researchers Supporting Project number (PNURSP2023R29), Princess Nourah bint Abdulrahman University, Riyadh, Saudi Arabia, the Office of Research and Sponsored Programs (ORSP) at Abu Dhabi University for funding this paper through a research fund.

Appendix A. Supplementary data

Supplementary data to this article can be found online at https://doi.org/10.1016/j.jpowsour.2023.233500.

References

[1] C. Zou, Q. Zhao, G. Zhang, B. Xiong, Energy revolution: from a fossil energy era to a new energy era, Nat. Gas. Ind. B 3 (2016) 1–11, https://doi.org/10.1016/j.ngib.2016.02.001.
[2] J. Kotcher, E. Maibach, W.-T. Choi, Fossil fuels are harming our brains: identifying key messages about the health effects of air pollution from fossil fuels, BMC Publ. Health 19 (2019) 1079, https://doi.org/10.1186/s12889-019-7373-1.
[3] S. Shafiee, E. Topal, When will fossil fuel reserves be diminished? Energy Pol. 37 (2009) 181–189, https://doi.org/10.1016/j.enpol.2008.08.016.
[4] A.G. Chmielewski, Environmental Effects of Fossil Fuel Combustion, Poland, 1999, pp. 1425–7351 [Online]. Available: http://inis.iaea.org/search/search.aspx?orig_q=RN:31003493.
[5] Y. Köysal, Performance analysis on solar concentrating thermoelectric generator coupled with heat sink, Int. J. Precis. Eng. Manuf. 20 (2019) 313–318, https://doi.org/10.1007/s12541-019-00060-w.
[6] R. Lamba, S. Manikandan, S.C. Kaushik, Performance analysis and optimization of concentrating solar thermoelectric generator, J. Electron. Mater. 47 (2018) 5310–5320, https://doi.org/10.1007/s11664-018-6410-7.
[7] J. Cao, X.Y. Tan, N. Jia, J. Zheng, S.W. Chien, H.K. Ng, et al., Designing good compatibility factor in segmented Bi0.5Sb1.5Te3 – GeTe thermoelectrics for high power conversion efficiency, Nano Energy 96 (2022), 107147, https://doi.org/10.1016/j.nanoen.2022.107147.
[8] N.K. Karri, C. Mo, Geometry optimization for structural reliability and performance of a thermoelectric generator, SN Appl. Sci. 1 (2019) 1097, https://doi.org/10.1007/s42452-019-1120-1.
[9] K. Cheng, J. Qin, Y. Jiang, S. Zhang, W. Bao, Performance comparison of single- and multi-stage onboard thermoelectric generators and stage number optimization at a large temperature difference, Appl. Therm. Eng. 141 (2018) 456–466, https://doi.org/10.1016/j.applthermaleng.2018.05.127.
[10] A.I. Alnahhal, A. Halal, B. Plesz, Thermal- electrical model of concentrated photovoltaic-thermoelectric generator combined system for energy generation, in: 2022 28th Int. Workshop Therm. Investig. ICs Syst. THERMINIC, IEEE, Dublin, Ireland, 2022, pp. 1–4, https://doi.org/10.1109/THERMINIC57263.2022.9950655.
[11] M.A. Al-Nimr, B.M. Tashtoush, M.A. Khasawneh, I. Al-Keyyam, A hybrid concentrated solar thermal collector/thermo-electric generation system, Energy 134 (2017) 1001–1012, https://doi.org/10.1016/j.energy.2017.06.093.
[12] H. Fagehi, A. Attar, H. Lee, Optimal design of an automotive exhaust thermoelectric generator, J. Electron. Mater. 47 (2018) 3983–3995, https://doi.org/10.1007/s11664-018-6282-x.
[13] R.R. Sahoo, D.R. Karana, Effect of design shape factor on exergonic performance of a new modified extended-tapering segmented thermoelectric generator system, Energy 200 (2020), 117561, https://doi.org/10.1016/j.energy.2020.117561.
[14] A.F. Ioffe, Semiconductor Thermoelements, and Thermoelectric Cooling. [Rev. and supplemented for the English, Infosearch, ltd, London, 1957.
[15] Y. Liu, B. Wang, K.F. Wang, J. Yang, Transient model and parameters matching of a segmented solar thermoelectric system, Int. J. Green Energy (2023) 1–14, https://doi.org/10.1080/15435075.2023.2200438.
[16] Y. Zhu, D.W. Newbrook, P. Dai, J. Liu, C.H.K. De Groot, R. Huang, Segmented thermoelectric generator modelling and optimization using artificial neural networks by iterative training, Energy AI 12 (2023), 100225, https://doi.org/10.1016/j.egyai.2022.100225.
[17] S. Shittu, G. Li, Q. Xuan, X. Zhao, X. Ma, Y. Cui, Electrical and mechanical analysis of a segmented solar thermoelectric generator under non-uniform heat flux, Energy 199 (2020), 117433, https://doi.org/10.1016/j.energy.2020.117433.
[18] J. Yu, L. Kong, Q. Zhu, H. Zhu, H. Wang, J. Guan, et al., Thermal stress analysis of a segmented thermoelectric generator under a pulsed heat source, J. Electron. Mater. 49 (2020) 4392–4402, https://doi.org/10.1007/s11664-020-08163-1.
[19] W.-H. Chen, Y.-B. Chiou, Geometry design for maximizing output power of segmented skutterudite thermoelectric generator by evolutionary computation, Appl. Energy 274 (2020), 115296, https://doi.org/10.1016/j.apenergy.2020.115296.
[20] C. Maduabuchi, H. Njoku, M. Eke, C. Mgbemene, R. Lamba, J.S. Ibrahim, Overall performance optimisation of tapered leg geometry based solar thermoelectric generators under isoflux conditions, J. Power Sources 500 (2021), 229989, https://doi.org/10.1016/j.jpowsour.2021.229989.
[21] C. Maduabuchi, Improving the performance of a solar thermoelectric generator using nano-enhanced variable area pins, Appl. Therm. Eng. 206 (2022), 118086, https://doi.org/10.1016/j.applthermaleng.2022.118086.
[22] M.A. Olivares-Robles, C.A. Badillo-Ruiz, P.E. Ruiz-Ortega, A comprehensive analysis on nanostructured materials in a thermoelectric micro-system based on geometric shape, segmentation structure and load resistance, Sci. Rep. 10 (2020), 21659, https://doi.org/10.1038/s41598-020-78770-9.
[23] H.-B. Liu, J.-H. Meng, X.-D. Wang, W.-H. Chen, A new design of solar thermoelectric generator with combination of segmented materials and

asymmetrical legs, Energy Convers. Manag. 175 (2018) 11–20, https://doi.org/10.1016/j.enconman.2018.08.095.

[24] S. Shittu, G. Li, X. Zhao, X. Ma, Y.G. Akhlaghi, E. Ayodele, Optimized high performance thermoelectric generator with combined segmented and asymmetrical legs under pulsed heat input power, J. Power Sources 428 (2019) 53–66, https://doi.org/10.1016/j.jpowsour.2019.04.099.

[25] Y.-Q. Zhang, J. Sun, G.-X. Wang, T.-H. Wang, Advantage of a thermoelectric generator with hybridization of segmented materials and irregularly variable cross-section design, Energies 15 (2022) 2944, https://doi.org/10.3390/en15082944.

[26] N. Espinosa, M. Lazard, L. Aixala, H. Scherrer, Modeling a thermoelectric generator applied to diesel automotive heat recovery, J. Electron. Mater. 39 (2010) 1446–1455, https://doi.org/10.1007/s11664-010-1305-2.